PMSTPCOL PEmails

From: Ballinger, Amy [aballinger@STPEGS.COM]
Sent: Wednesday, July 09, 2008 5:39 PM
To: George Wunder
Cc: Raj Anand; Mookhoek, William; Chappell, Coley
Subject: Response to Requests for Additional Information
Attachments: ABR-AE-08000050.pdf

Mr. Wunder,

Please find attached a courtesy electronic copy of an RAI response letter with attachments.
On July 09, 2008, an official paper copy was sent by overnight delivery to your address.

Amy Ballinger
STP Units 3 & 4
Licensing Specialist
Phone: (361)972-4644
Fax: (361) 972-4751

Hearing Identifier: SouthTexas34Public_EX
Email Number: 93

Mail Envelope Properties (3AACB39ACCF95E46A44EED875EEA677005C0C056)

Subject: Response to Requests for Additional Information
Sent Date: 7/9/2008 5:39:00 PM
Received Date: 7/9/2008 5:40:00 PM
From: Ballinger, Amy

Created By: aballinger@STPEGS.COM

Recipients:
"Raj Anand" <Raj.Anand@nrc.gov>
Tracking Status: None
"Mookhoek, William" <wemookhoek@STPEGS.COM>
Tracking Status: None
"Chappell, Coley" <ccchappell@STPEGS.COM>
Tracking Status: None
"George Wunder" <George.Wunder@nrc.gov>
Tracking Status: None

Post Office: exgbe1.corp.stpegs.net

Files	**Size**	**Date & Time**
MESSAGE	321	7/9/2008 5:40:00 PM
ABR-AE-08000050.pdf	1605339	

Options
Priority: Standard
Return Notification: No
Reply Requested: No
Sensitivity: Normal
Expiration Date:
Recipients Received:

Nuclear Operating Company

South Texas Project Electric Generating Station 4000 Avenue F – Suite A Bay City, Texas 77414

July 9, 2008
ABR-AE-08000050

U. S. Nuclear Regulatory Commission
Attention: Document Control Desk
One White Flint North
11555 Rockville Pike
Rockville MD 20852-2738

South Texas Project
Units 3 and 4
Docket Nos. 52-012 and 52-013
<u>Response to Requests for Additional Information</u>

Attached are responses to NRC staff questions included in Request for Additional Information (RAI) letter numbers 31, 32, 39, 42, 49, 50, and 52 related to Combined License Application (COLA) Part 2, Tier 2 Sections 2.4S and 2.5S. This submittal includes responses to the following Question numbers:

02.04.01-2	02.04.12-2	02.05.01-11	02.05.02-1	02.05.04-5
02.04.02-4	02.04.12-7	02.05.01-16	02.05.02-2	02.05.04-6
02.04.03-6	02.04.12-9		02.05.02-3	02.05.04-7
	02.04.12-13		02.05.02-4	02.05.04-8
			02.05.02-6	
			02.05.02-7	

When a change to the COLA is indicated by a question response, the change will be incorporated into the next routine revision of the COLA following NRC acceptance of the question response.

There are no new commitments made in this letter.

If you have any questions regarding the attached responses, please contact me at (361) 972-4626, or Bill Mookhoek at (361)-972-7274.

I declare under penalty of perjury that the foregoing is true and correct.

Executed on July 9, 2008

Gregory T. Gibson
Manager, Regulatory Affairs
South Texas Project Units 3 & 4

ccc

Attachments:
1. Question 02.04.01-2
2. Question 02.04.02-4
3. Question 02.04.03-6
4. Question 02.04.12-2
5. Question 02.04.12-7
6. Question 02.04.12-9
7. Question 02.04.12-13
8. Question 02.05.01-11
9. Question 02.05.01-16
10. Question 02.05.02-1
11. Question 02.05.02-2
12. Question 02.05.02-3
13. Question 02.05.02-4
14. Question 02.05.02-6
15. Question 02.05.02-7
16. Question 02.05.04-5
17. Question 02.05.04-6
18. Question 02.05.04-7
19. Question 02.05.04-8

cc: w/o attachment except*

(paper copy)

Director, Office of New Reactors
U. S. Nuclear Regulatory Commission
One White Flint North
11555 Rockville Pike
Rockville, MD 20852-2738

Regional Administrator, Region IV
U. S. Nuclear Regulatory Commission
611 Ryan Plaza Drive, Suite 400
Arlington, Texas 76011-8064

Richard A. Ratliff
Bureau of Radiation Control
Texas Department of State Health Services
1100 West 49th Street
Austin, TX 78756-3189

C. M. Canady
City of Austin
Electric Utility Department
721 Barton Springs Road
Austin, TX 78704

*Steven P. Frantz, Esquire
A. H. Gutterman, Esquire
Morgan, Lewis & Bockius LLP
1111 Pennsylvania Ave. NW
Washington D.C. 20004

*George F. Wunder
Two White Flint North
11545 Rockville Pike
Rockville, MD 20852

*Raj Anand
Two White Flint North
11545 Rockville Pike
Rockville, MD 20852

(electronic copy)

*George Wunder
Loren R. Plisco
U. S. Nuclear Regulatory Commission

Brad Porlier
Steve Winn
Eddy Daniels
NRG South Texas 3/4 LLC

Jon C. Wood, Esquire
Cox Smith Matthews

J. J. Nesrsta
R. K. Temple
Kevin Pollo
L. D. Blaylock
CPS Energy

RAI 02.04.01-2:

QUESTION:

Summarize in Section 2.4S.1 of the FSAR: (a) plant water demands in accordance with SRP 2.4.1 and (b) the geo-referencing datum used throughout Section 2.4S.

RESPONSE:

Part (a) Response:
The plant water demands are provided in the Environmental Report of the STP Units 3 & 4 COLA (Part 3, Section 3.3). The consumption of plant water for STP Units 3 & 4 will closely resemble practices currently followed by STP Units 1 & 2. Surface water makeup demand for the MCR is approximately 43,000 gpm, with a maximum of approximately 45,000 gpm. The UHS makeup well water demand is approximately 700 gpm, with a maximum of approximately 3,000 gpm. The total plant makeup well water demand (including UHS) is approximately 1,100 gpm on average, with a maximum of approximately 4,000 gpm.

The following paragraph will be added at the end of Section 2.4S.1.2.1.5, "Surface Water Use:"

> The plant water water demands for STP Units 3 & 4 are located in Table 3.3-1 of the Environmental Report. The total surface water demand for STP Units 3 & 4 is given by Stream 3, Total Required River Water to MCR. The plant requires surface water consumption only for MCR makeup.

The following paragraph will be added at the end of Section 2.4S.1.2.2, "Groundwater:"

> The plant water demands for STP Units 3 & 4 are located in Table 3.3-1 of the Environmental Report. The total ground (well) water demand for STP Units 3 & 4 is given by Stream 2, Plant Well Water Demand. The plant requires well water makeup for Power Plant Makeup/Use, UHS System Makeup, and Potable Water.

Part (b) Response:

Section 2.4S adopts the National Geodetic Vertical Datum of 1929 (NGVD 29) as the referenced datum for all vertical elevations, including surface water elevations and topographic elevations. For STP 3 & 4, the convention MSL, which is equivalent to NGVD29, is also used. There are a few exceptions when a subsection made reference to, and used as input data from, hydrologic studies conducted by others for flood levels and elevation information that were tied to the North American Vertical Datum of 1988 (NAVD88). In these few occasions, the original datum from the cited studies is identified. Because the elevation difference between the two datums, NGVD29 (or MSL) and NAVD88, is small, about 0.16 ft near the site, not all elevations referenced in NAVD88 have been converted to NGVD29. However, the resulting flood levels or low water elevation analyzed and presented in Section 2.4S are reported in NGVD29 (or MSL).

A search of the COLA will be performed for references to vertical survey datums and clarifications or revisions will be made to include the NGVD29 values, where appropriate, in a future revision of the COLA.

For item (b), the first paragraph of Subsection 2.4S.1.1 will be separated into two paragraphs and revised as follows to identify the geo-referencing datum used throughout Section 2.4S:

> The STP 3 & 4 site is located in Matagorda County, Texas, near the west bank of the Colorado River, opposite river mile 14.6. It is approximately 12 miles south-southwest of Bay City, Texas, and 8 miles north-northwest of Matagorda, Texas (Figure 2.4S.1-1). The surface elevation of the site ranges from about El. 32 to 34 ft mean sea level (MSL), which is equivalent to National Geodetic Vertical Datum of 1929 (NGVD 29), at the north boundary to between El. 15 to 20 ft MSL at the south ~~end~~ boundary. ~~The nominal plant grade elevation is 34 ft MSL and the entrance level grade elevation of the safety-related facilities is 35 ft MSL.~~
>
> Figure 2.4S.1-2 shows the topography and hydrologic features within about 3 miles from the site based on digital data from the U.S. Geological Survey (USGS). Figure 2.4S.1-3 shows the existing (predevelopment) topography of the site in more detail based on data from a recent aerial survey. Figure 2.4S.1-3 also shows various external plant structures and components. The proposed site layout and drainage system after the construction of Unit 3 & 4 is discussed in Subsection 2.4S.2. The post-development topography and major drainage features of the site are presented in Figure 2.4S.2-4.

RAI 02.04.02-4:

<u>QUESTION</u>:

Provide elaboration of the following statements in FSAR, Revision 0, Section 2.4S.2.3.4, page 2.4S.2-8: “The peak discharge obtained for a subbasin in HEC-HMS was first distributed to the most upstream cross section of a stream reach in HEC-RAS in proportion to the area contributing to that cross section and the total area of the subbasin. The remaining portion of the peak discharge is then distributed equally among the remaining cross sections within the receiving channel reach.” The staff needs this information to understand the procedure used to evaluate its degree of conservatism.

<u>RESPONSE</u>:

The inflow to each of the modeled river/channel cross-sections (CS) in the HEC-RAS simulation was derived from the flood flow hydrographs computed using the HEC-HMS model for the seven contributing subbasins as described below. The designations of the drainage elements, i.e., the subbasins, storage area, and channels, are shown in FSAR Figure 2.4S.2-6.

Table 1 lists the incremental flood flow and the cumulative discharge at each of the HEC-RAS modeled cross sections. Based on the topographic features and the layout of the plant, the contributing drainage area that has a potential to affect flood level at the power block is delineated into 2 groups of subbasins: subbasins near the power block (PBW, PBW1, PBE and PBN1) and subbasins to the west of the power block (North1, North2 and North3). Due to the differences in the drainage areas, lengths of flow paths and travel times between the 2 groups of subbasins, the peak of the respective flood hydrographs predicted by HEC-HMS arrive at times that are substantially different. The flood hydrographs of PBW, PBW1, PBE and PBN1 peak at around 3 hr 10 min to 3 hr 35 min into the storm, which is close to the 03:35 hr arrival time of the peak of the outflow hydrograph at the downstream-most junction in the HEC-HMS model. The peaks of the flood hydrographs of North1, North2, which are routed through the storage area US LRS, and North3, however, arrive much later. In the HEC-RAS simulation, it is postulated that the peak discharge from each of the power block subbasins would arrive at the same time, which is chosen to be 03:35 hr into the storm. The outflow from the storage area US LRS and the flood discharge of subbasin North3 at 03:35 hr model time are used as inflow to the corresponding HEC-RAS channel cross-sections, as discussed in FSAR Subsection 2.4S.2.3.4 (page 2.4S.2-8).

West of the power block, the combined flood flow of 905.3 cfs from subbasins North1 and North2 at 03:35 hr is routed through the storage area US LRS and discharges at the upstream-most cross section of Little Robbins Slough (LRS). The flood flow of 815.9 cfs from the hydrograph of subbasin North3 at 03:35 hr is allocated equally between the 11 HEC-RAS cross sections used to represent LRS. Therefore, the inflow at the upstream-most cross section, CS 2200, of LRS is the sum of the outflow from US LRS and the flood discharge from North3, which is about 979.5 cfs (905.3 + 815.9/11 cfs). At the next cross section downstream, CS 2000, the discharge is increased to 1053.6 cfs by an incremental inflow of 815.9/11 cfs. Repeating the same process along the remaining cross sections of LRS, the flow discharge at the downstream-most cross section, CS 0200, is 1721.2 cfs, which is equal to the total discharge of US LRS and North3 (905.3+815.9 cfs) at 03:35 hr.

Near the power block, an area of approximately 0.1 mi^2 of subbasin PBN1, located east of the plant approach road, would drain to the upstream-most cross section of the Main Drainage Channel (MDC). The peak discharge from this area, prorated from the flood peak of 4243.8 cfs for the total area of 0.319 mi^2 of subbasin PBN1, is about 1330.3 cfs (0.1/0.319 x 4243.8 cfs). This prorated flood peak is provided as an inflow to the upstream-most cross section, CS 5380, of the MDC. The remaining discharge from PBN1 is allocated between the two channel segments of the MDC, from CS 5200 to CS 2200 and from CS 2000 to CS 0000, based on the contributing drainage areas of the segments. Within each of these two channel segments, the incremental discharge is allocated equally among the cross sections. The peak discharge from subbasin PBW1 (1367.7 cfs) is provided as a point inflow to the MDC at CS 1200 to represent the small stream that carries the flood flow from PBW1 and joins the MDC just upstream of the cross section location. Contribution from LRS is added to the MDC at CS 0400.

For the East and West Channels (EC and WC, respectively), inflow at the upstream-most cross section is provided based on the peak discharge prorated in accordance with the ratio of the drainage area associated with the cross section and the total area of the subbasin. The remaining discharge is allocated equally to each of the downstream cross sections as incremental inflow.

No incremental inflow is allocated to the interpolated cross sections and inline structures. The discharge at these sections is taken as the channel flow from the cross section immediately upstream.

The total allocated discharge at the outflow location (MDC CS 0000) simulated in the HEC-RAS model is 11,080.4 cfs, which is larger, and therefore more conservative, than the peak flow rate of 9852.0 cfs (occurs at 3:35 hrs into the storm) predicted by the HEC-HMS.

No COLA revision is required as a result of this RAI response.

Table 1 – HEC-RAS Inflow Discharges for Different Cross Sections (River Stations)

Channel	Reach	River Station	Downstream Reach Length (ft)	Contributing Subbasins	Incremental Inflow (cfs)	Model Discharge in HEC-RAS (cfs)	Comments
EastChannel	EC-R1	1690	90	PBE	632.5	632.5	Upstream CS
EastChannel	EC-R1	1600	200		90.1	722.6	
EastChannel	EC-R1	1400	200		90.1	812.6	
EastChannel	EC-R1	1200	200		90.1	902.7	
EastChannel	EC-R1	1000	200		90.1	992.8	
EastChannel	EC-R1	0800	200		90.1	1082.9	
EastChannel	EC-R1	0600	200		90.1	1173.0	
EastChannel	EC-R1	0400	200		90.1	1263.1	
EastChannel	EC-R1	0200	100		90.1	1353.2	
EastChannel	EC-R1	0150	In-line Structure				
EastChannel	EC-R1	0050	0		90.1	1443.3	
LRS	LRS-R1	2200	200	North1, North2, North3[a]	979.5	979.5	From US LRS[a]
LRS	LRS-R1	2000	200		74.2	1053.6	
LRS	LRS-R1	1800	200		74.2	1127.8	
LRS	LRS-R1	1600	200		74.2	1202.0	
LRS	LRS-R1	1400	200		74.2	1276.2	
LRS	LRS-R1	1200	200		74.2	1350.3	
LRS	LRS-R1	1000	200		74.2	1424.5	
LRS	LRS-R1	0800	200		74.2	1498.7	
LRS	LRS-R1	0600	200		74.2	1572.9	
LRS	LRS-R1	0400	200		74.2	1647.0	
LRS	LRS-R1	0200	0		74.2	1721.2	

Table 1 – HEC-RAS Inflow Discharges for Different Cross Sections (River Stations) (continued)

Channel	Reach	River Station	Downstream Reach Length (ft)	Contributing Subbasins	Incremental Inflow (cfs)	Model Discharge in HEC-RAS (cfs)	Comments
MDC	MDC-R1	5380	100	PBE, PBW, PBN1, PBW1	1330.3	1330.3	Upstream CS
MDC	MDC-R2	5200	200		144.7	2918.3	EC flow added
MDC	MDC-R2	5000	200		144.7	3063.0	
MDC	MDC-R2	4800	200		144.7	3207.7	
MDC	MDC-R2	4600	200		144.7	3352.3	
MDC	MDC-R2	4400	200		144.7	3497.0	
MDC	MDC-R2	4200	200		144.7	3641.7	
MDC	MDC-R2	4000	200		144.7	3786.4	
MDC	MDC-R2	3800	200		144.7	3931.0	
MDC	MDC-R2	3600	200		144.7	4075.7	
MDC	MDC-R2	3400	0		144.7	4220.4	
MDC	MDC-R3	3200	200		144.7	6669.5	WC flow added
MDC	MDC-R3	3000	200		144.7	6814.1	
MDC	MDC-R3	2800	200		144.7	6958.8	
MDC	MDC-R3	2600	200		144.7	7103.5	
MDC	MDC-R3	2400	200		144.7	7248.2	
MDC	MDC-R3	2200	200		144.7	7392.8	
MDC	MDC-R3	2000	200		54.4	7447.3	
MDC	MDC-R3	1800	200		54.4	7501.7	
MDC	MDC-R3	1600	200		54.4	7556.1	
MDC	MDC-R3	1400	200		54.4	7610.5	

Table 1 – HEC-RAS Inflow Discharges for Different Cross Sections (River Stations) (continued)

Channel	Reach	River Station	Downstream Reach Length (ft)	Contributing Subbasins	Incremental Inflow (cfs)	Model Discharge in HEC-RAS (cfs)	Comments
MDC	MDC-R3	1200	200		54.4	9032.7	PBW1 flow added
MDC	MDC-R3	1000	200		54.4	9087.1	
MDC	MDC-R3	0800	200		54.4	9141.5	
MDC	MDC-R3	0600	0		54.4	9195.9	
MDC	MDC-R4	0400	200		54.4	10971.6	LRS flow added
MDC	MDC-R4	0200	100		54.4	11026.0	
MDC	MDC-R4	0050	In-line Structure				
MDC	MDC-R4	0000	0		54.4	11080.4	
WestChannel	WC-R1	1690	90	PBW	472.8	472.8	Upstream CS
WestChannel	WC-R1	1600	200		203.5	676.3	
WestChannel	WC-R1	1400	200		203.5	879.8	
WestChannel	WC-R1	1200	200		203.5	1083.4	
WestChannel	WC-R1	1000	200		203.5	1286.9	
WestChannel	WC-R1	0800	200		203.5	1490.4	
WestChannel	WC-R1	0600	200		203.5	1693.9	
WestChannel	WC-R1	0400	200		203.5	1897.4	
WestChannel	WC-R1	0200	100		203.5	2100.9	
WestChannel	WC-R1	0150	In-line Structure				
WestChannel	WC-R1	0050	0		203.5	2304.4	

[a] Inflow corresponding to 03:35 hrs into the storm

RAI 02.04.03-6:

QUESTION:

In FSAR Section 2.4S.3.5.3.1, explain why the water level in the Colorado River at the downstream most cross-section used in the HEC-RAS model is unaffected by tidal conditions.

RESPONSE:

Under Probable Maximum Flood (PMF) conditions, the water level in the downstream-most cross-section (RS 383+64.5) of the Halff study (Reference 2.4S.3-8) is not controlled by tidal effects. As shown in Figure 2.4S.3-11 and discussed in Section 2.4S.3.5.3.1, the normal depth for the PMF discharge of 1,397,432 cfs at the downstream boundary (RS 383+64.5) was estimated to be equal to 17.5 ft NAVD88 (17.7 ft NGVD 29). The highest water level recorded for National Oceanic and Atmospheric Administration (NOAA) Station #8772440 at Freeport, Texas, is 4.95 feet above mean sea level (MSL) (Reference 2.4S.3-XX). Because the water surface elevation for the PMF with a normal depth condition exceeds the water surface elevation for the maximum tidal level, the normal depth condition is the appropriate boundary condition.

The first paragraph in FSAR Section 2.4S.3.5.3.1 of the COLA will be revised as follows:

> Under PMF flow conditions, the water level in the river at the downstream-most cross-section (RS 383+64.5) is not ~~influenced~~controlled by tidal effects. From 1961 to 2001, the highest water level recorded for National Oceanic and Atmospheric Administration (NOAA) Station #8772440 at Freeport is 4.95 feet above mean sea level (MSL) (Reference 2.4S.3-XX). Therefore, normal depth for an estimated channel slope of 0.0001 is an appropriate boundary condition to use at the downstream-most cross-section of the model that is located approximately 7.3 mile upstream from the shoreline of the Gulf of Mexico (see Table 2.4S.4.3-7).

The following reference will be added to FSAR Section 2.4S.3:

2.4S.3-XX “NOAA Tides and Currents”, Station #8772440, Available at http://www.co-ops.nos.noaa.gov/data_menu.shtml?stn=8772440%20Freeport,%20TX&type=Datums, accessed May 23, 2008.

RAI 02.04.12-2:

QUESTION:

The depths to and thicknesses of hydrogeologic units described in 2.4S.12.1.3 are not the same as those shown in Figure 2.4S.12-29 and Table 2.4S.12-14. There is a similar inconsistency on Page 2.4S.12-10, Section 2.4S.12.2.2 for the 0.06 to 0.29 downward hydraulic gradient. Please clarify or resolve these inconsistencies.

RESPONSE:

FSAR Section 2.4S.12.1.3 refers to the generalized local, not site-specific, hydrostratigraphy. Since Figure 2.4S.12-29 and Table 2.4S.12-14 represent generalized site-specific data (with respect to depths and thicknesses), the text describing the local hydrogeology may not necessarily agree with the site-specific data as geologic units vary in thickness and depth with location.

The text on page 2.4S.12-10, Section 2.4S.12.2.2.2 of the FSAR accurately reports (albeit, rounded numbers) what is presented in Table 2.4S.12-8 (which has been verified as correct). However, in Table 2.4S.12-14, the low range figure of 0.079 should be 0.063 (before rounding).

The following change to FSAR Table 2.4S.12-14 will be made:

Hydrogeologic Unit	Property	Units	Representative Value	Range	Source
Upper Shallow Aquifer Confining Layer	Thickness	ft	20	10-30	Figure 2.4S.12-20
	Vertical Hydraulic Conductivity	gpd/ft^2	0.004	0.05-0.0005	Table 2.4S.12-13
	Bulk (dry) Density	pcf	101	96.4 - 114.9	Table 2.4S.12-12
	Total Porosity	%	40	31.8-42.8	Table 2.4S.12-12
Upper Shallow Aquifer	Thickness	ft	25	20-30	Figure 2.4S.12-20
	Horizontal Hydraulic Conductivity	gpd/ft^2	192	39-561	Table 2.4S.12-11
	Hydraulic Gradient	ft/ft	0.002	0.001-0.002	Section 2.4S.12.2.2
	Bulk (dry) Density	pcf	99	97.2 - 100.2	Table 2.4S.12-12
	Total Porosity	%	41	39.5-41.7	Table 2.4S.12-12
	Effective Porosity	%	33	31.6-33.4	Table 2.4S.12-12
Lower Shallow Aquifer Confining Layer	Thickness	ft	20	15-25	Figure 2.4S.12-20
	Vertical Hydraulic Gradient	ft/ft	0.29	~~0.079~~ 0.063-0.29	Table 2.4S.12-8
	Vertical Hydraulic Conductivity	gpd/ft^2	0.004	0.05-0.0005	Table 2.4S.12-13
	Bulk (dry) Density	pcf	99	87.3 - 107.7	Table 2.4S.12-12
	Total Porosity	%	42	36.1-47.2	Table 2.4S.12-12
Lower Shallow	Thickness	ft	40	25-50	Figure 2.4S.12-20

Aquifer	Horizontal Hydraulic Conductivity	gpd/ft^2	543	410-651	Table 2.4S.12-10
	Hydraulic Gradient	ft/ft	0.0004	0.0004	Section 2.4S.12.2.2
	Bulk (dry) Density	pcf	102	94.5 - 120.0	Table 2.4S.12-12
	Total Porosity	%	39	28.8-43.9	Table 2.4S.12-12
	Effective Porosity	%	31	23.0-35.1	Table 2.4S.12-12
Deep Aquifer Confining Layer	Thickness	ft	100	100-150	Section 2.4S.12.3.1
	Vertical Hydraulic Conductivity	gpd/ft^2	0.004	0.05-0.0005	Table 2.4S.12-13
	Bulk (dry) Density	pcf	101	82.1 - 111.4	Table 2.4S.12-12
	Total Porosity	%	41	33.4 - 51.8	Table 2.4S.12-12
Deep Aquifer	Horizontal Hydraulic Conductivity	gpd/ft^2	420	103-3,950	Table 2.4S.12-9
	Horizontal Hydraulic Gradient	ft/ft	0.002	0.0006-0.002	Section 2.4S.12.2.2
	Bulk (dry) Density	pcf	102	94.5 - 120.0	Lower Shallow Aquifer
	Total Porosity	%	39	28.8-43.9	Lower Shallow Aquifer
	Effective Porosity	%	31	23.0-35.1	Lower Shallow Aquifer

RAI 02.04.12-7:

<u>QUESTION</u>:

In FSAR Section 2.4S.12.2.3, "Temporal Groundwater Trends", is the recovery seen in data from Well 8015402 typical of the groundwater resource in the region or is it a local phenomenon? Does this reflect a regional trend toward lower groundwater resource usage? Does this align with the forecast by the TWDB in 1985 that groundwater resource use in Matagorda County would drop by 48% by 2030? How does this align with the annual data on groundwater use in the county reported in Table 2.4S.12-5? They appear contradictory. Please clarify.

<u>RESPONSE</u>:

The data illustrated by FSAR Figure 2.4S.12-22 was presented to show historic potentiometric surface conditions from regional wells in the site vicinity as required by Regulatory Guide (RG) 1.206, Section C.I.2.4.12.2. This presentation was intended to evaluate the portion of the county in the vicinity of the site rather than the entire county. Consequently, data from the two wells screened in different portions of the Deep Aquifer were presented, as this is the most widely used aquifer in this portion of the county. The trend from these wells represents local phenomena in the vicinity of these regional wells. Data from other wells in the county were considered in the evaluation of regional groundwater use patterns discussed in the FSAR 2.4S.12 sections leading up to 2.4S.12.2.3.

Regional, historical surface water and groundwater use data obtained from the TWDB for Matagorda County are summarized in Table 2.4S.12-5. These data show a steady groundwater withdrawal rate in the county from 1974 (41,159 acre-feet) to 1984 (39,556 acre-feet). A subsequent period of fluctuating groundwater use from 1984 to 1996 (37,557 acre-feet) is followed by a relatively short period of decline to 1999 (15,087 acre-feet). The trend from 1999 to 2004 (45,693 acre-feet) may actually represent a return to historic withdrawals following a period of decline. Consequently, the recent apparent increase in groundwater withdrawal in the county between 1999 and 2004 may not necessarily contradict the forecasted 48 percent decline, but a return to an interim period of fluctuation. Additionally, the overall county trend summarized in Table 2.4S.12-5 represents the monitored groundwater withdrawals, and is not explicitly representative of the zone of the Deep Aquifer or geographic location represented by Well 8015402. Considering the two datasets do not represent the same phenomenon, their trends are not necessarily contradictory.

The following revision will be made to the first paragraph of FSAR Section 2.4S.12.2.3.

The TWDB has collected groundwater level data in Matagorda County since the 1930s (Reference 2.4S.12-16). Two observation wells near the STP were selected to prepare the regional hydrographs in the vicinity of the site, shown on Figure 2.4S.12-22. These wells monitor two different intervals in the Deep Aquifer. Well 8015402 monitors the heavy pumping interval at about 300 ft below ground surface. This well indicates that between 1957 and the early 1990s, a significant drop in groundwater level occurred. Since the early 1990s, the groundwater level has been recovering and has nearly returned to the 1957 level. The second well, 8015301, monitors the deeper zone of the Deep Aquifer, corresponding to the production zone in the STP onsite wells (well depths from 600 ft to 700 ft below ground surface). This well shows generally stable water levels over the period of record for the well. Due to the limited groundwater development potential in the Shallow Aquifer, regional temporal measurements of water levels have not been collected.

RAI 02.04.12-9:

<u>QUESTION</u>:

In FSAR Section 2.4S.12.2.3, “Temporal Groundwater Trends”, the applicant acknowledges the groundwater field observations do not span a full year and therefore, do not provide the seasonal data required in the application. Provide the seasonal data set.

<u>RESPONSE</u>:

A full year of monthly water level measurements from the Units 3 & 4 Upper and Lower Shallow Aquifer wells was completed on December 17, 2007. The monthly 2007 data are now available. A table of these readings is provided with this response.

The third paragraph of FSAR Section 2.4S.12.2.3 will be revised to include a statement that one year of water level measurements has now been collected.

> Shallow Aquifer observation wells installed as part of the STP 3 & 4 subsurface investigation program have been used for monthly water level measurements ~~since~~ from December of 2006~~. Monthly groundwater levels will be collected~~ through December 2007~~ from the STP 3 & 4 observation wells~~. Confirmatory information, based on the additional water level measurements, will be provided in a future COLA update in accordance with 10CFR50.71(e) (COM 2.4S-2). Three well series designations represent the following location areas.
>
> - OW-300 series wells are located in the proposed STP 3 facility area.
> - OW-400 series wells are located in the proposed STP 4 facility area.
> - OW-900 series wells include all of the wells located outside of the power block areas.

WELL ID	WELL DEPTH	BOTTOM OF SCREEN	REFERENCE POINT ELEVATION	December 28, 2006		January 30, 2007		February 22, 2007		March 29, 2007		April 27, 2007		May 25, 2007		June 27, 2007		July 30, 2007		August 30, 2007 (2)		September 26, 2007		October 30, 2007		November 19, 2007		December 17, 2007	
	(ft bgs)	(ft bgs)	(ft)	Depth to Water (ft)	Elevation (ft msl)	Depth to Water (ft)	Elevation (ft msl)	Depth to Water (ft)	Elevation (ft msl)	Depth to Water (ft)	Elevation (ft msl)	Depth to Water (ft)	Elevation (ft msl)	Depth to Water (ft)	Elevation (ft msl)	Depth to Water (ft)	Elevation (ft msl)	Depth to Water (ft)	Elevation (ft msl)	Depth to Water (ft)	Elevation (ft msl)	Depth to Water (ft)	Elevation (ft msl)	Depth to Water (ft)	Elevation (ft msl)	Depth to Water (ft)	Elevation (ft msl)	Depth to Water (ft)	Elevation (ft msl)
Shallow Aquifer - Upper Zone																													
OW-308 U	47.1	46	31.80	7.78	24.02	6.46	25.34	7.46	24.34	7.41	24.39	7.17	24.63	7.07	24.73	7.72	24.08	6.36	25.44	7.30	24.50	7.50	24.30	8.09	23.71	8.40	23.40	8.23	23.57
OW-332 U	46.1	45	32.10	8.01	24.09	6.57	25.53	7.46	24.64	7.39	24.71	6.25	25.85	7.09	25.01	8.05	24.05	6.50	25.60	7.40	24.70	7.65	24.45	8.43	23.67	8.80	23.30	8.60	23.50
OW-348 U	39.1	38	32.28	8.09	24.19	6.52	25.76	7.71	24.57	7.66	24.62	7.34	24.94	7.25	25.03	7.95	24.33	6.34	25.94	7.50	24.78	7.78	24.50	8.42	23.86	8.79	23.49	8.56	23.72
OW-349 U	46.1	45	31.29	7.28	24.01	5.82	25.47	6.97	24.32	6.91	24.38	6.56	24.73	6.50	24.79	7.19	24.10	5.62	25.67	6.70	24.59	6.98	24.31	7.61	23.68	7.97	23.32	7.75	23.54
OW-408 U	43.1	42	33.57	9.71	23.86	8.30	25.27	9.13	24.44	9.08	24.49	8.95	24.62	8.94	24.63	9.47	24.10	8.19	25.38	6.10	27.47	9.28	24.29	9.81	23.76	10.23	23.34	10.12	23.45
OW-420 U	49.1	48	33.79	9.98	23.81	8.42	25.37	9.32	24.47	9.26	24.53	9.08	24.71	8.99	24.80	9.59	24.20	8.23	25.56	6.20	27.59	9.45	24.34	10.15	23.64	10.48	23.31	10.33	23.46
OW-438 U	41	40	32.18	8.45	23.73	6.55	25.63	7.21	24.97	7.14	25.04	7.17	25.01	7.00	25.18	7.97	24.21	6.32	25.86	7.40	24.78	7.55	24.63	8.54	23.64	8.98	23.20	8.88	23.30
OW-910 U	36.1	35	32.32	9.11	23.21	7.57	24.75	8.30	24.02	8.23	24.09	8.10	24.22	8.00	24.32	8.49	23.83	7.53	24.79	8.40	23.92	8.50	23.82	9.29	23.03	9.52	22.80	9.41	22.91
OW-928 U	39.6	38.5	31.69	8.18	23.51	6.21	25.48	6.85	24.84	6.72	24.97	6.69	25.00	6.59	25.10	7.33	24.36	6.09	25.60	6.95	24.74	7.22	24.47	8.31	23.38	8.64	23.05	8.52	23.17
OW-929 U	60.1	59	38.71	12.92	25.79	11.33	27.38	11.68	27.03	11.75	26.96	11.77	26.94	11.81	26.90	13.17	25.54	11.22	27.49	12.15	26.56	12.20	26.51	13.73	24.98	14.73	23.98	14.19	24.52
OW-930 U	36.1	35	27.33	7.92	19.41	5.79	21.54	7.05	20.28	6.98	20.35	6.45	20.88	7.31	20.02	7.97	19.36	6.09	21.24	7.10	20.23	8.05	19.28	8.62	18.71	8.39	18.94	8.35	18.98
OW-931 U	36	35	32.10	9.82	22.28	8.81	23.29	9.43	22.67	9.34	22.76	9.19	22.91	9.25	22.85	9.33	22.77	9.00	23.10	9.30	22.80	9.60	22.50	10.14	21.96	10.13	21.97	10.00	22.10
OW-932 U	39.6	38.5	32.83	8.52	24.31	7.03	25.80	8.04	24.79	7.96	24.87	7.77	25.06	7.68	25.15	8.27	24.56	6.94	25.89	7.90	24.93	8.20	24.63	8.76	24.07	9.04	23.79	8.83	24.00
OW-933 U	37.1	36	30.62	6.44	24.18	4.97	25.65	5.95	24.67	5.91	24.71	5.57	25.05	5.50	25.12	5.87	24.75	4.61	26.01	5.40	25.22	5.80	24.82	6.42	24.20	6.78	23.84	6.60	24.02
OW-934 U	41.1	40	30.39	10.22	20.17	9.54	20.85	10.04	20.35	10.08	20.31	9.91	20.48	10.00	20.39	10.36	20.03	9.56	20.83	10.00	20.39	10.15	20.24	10.60	19.79	10.55	19.84	10.55	19.84
Shallow Aquifer - Lower Zone																													
OW-308 L	97.1	96	31.78	16.08	15.70	15.08	16.70	14.91	16.87	14.67	17.11	14.21	17.57	14.32	17.46	14.30	17.48	12.95	18.83	13.40	18.38	13.60	18.18	14.20	17.58	14.60	17.18	14.80	16.98
OW-332 L (1)	103.2	102.1	31.85	15.22	16.63																								
OW-332 L (R)	103.1	102	32.08					15.29	16.79	15.05	17.03	14.59	17.49	14.71	17.37	14.68	17.40	13.32	18.76	13.80	18.28	13.95	18.13	14.58	17.50	14.99	17.09	15.17	16.91
OW-348 L	79.1	78.2	31.86	16.16	15.70	15.08	16.78	14.94	16.92	14.71	17.15	14.29	17.57	14.40	17.46	14.36	17.50	13.05	18.81	13.50	18.36	13.65	18.21	14.25	17.61	14.67	17.19	14.87	16.99
OW-349 L	81.1	80	31.03	15.22	15.81	14.19	16.84	14.02	17.01	13.80	17.23	13.35	17.68	13.48	17.55	13.42	17.61	12.05	18.98	12.50	18.53	12.72	18.31	13.32	17.71	13.74	17.29	13.94	17.09
OW-408 L	81.3	80.2	33.76	18.05	15.71	17.05	16.71	16.86	16.90	16.64	17.12	16.20	17.56	16.32	17.44	16.28	17.48	14.96	18.80	15.40	18.36	15.58	18.18	16.17	17.59	16.58	17.18	16.77	16.99
OW-438 L	104.1	103	31.57	15.85	15.72	14.96	16.61	14.75	16.82	14.49	17.08	14.02	17.55	14.12	17.45	14.10	17.47	12.79	18.78	13.20	18.37	13.40	18.17	13.98	17.59	14.37	17.20	14.55	17.02
OW-910 L	92.1	91	32.48	16.62	15.86	16.22	16.26	15.77	16.71	15.59	16.89	15.27	17.21	15.22	17.26	15.13	17.35	14.49	17.99	14.45	18.03	14.50	17.98	14.76	17.72	14.99	17.49	15.17	17.31
OW-928 L	121.1	120	31.56	15.75	15.81	15.00	16.56	14.75	16.81	14.50	17.06	14.03	17.53	14.13	17.43	14.06	17.50	12.90	18.66	13.25	18.31	13.35	18.21	13.90	17.66	14.25	17.31	14.41	17.15
OW-929 L	98.1	97	38.63	23.47	15.16	22.41	16.22	22.26	16.37	22.00	16.63	21.51	17.12	21.70	16.93	21.67	16.96	20.18	18.45	20.75	17.88	20.95	17.68	21.63	17.00	22.04	16.59	22.21	16.42
OW-930 L	106.5	105	27.98	14.90	13.08	13.41	14.57	13.35	14.63	13.21	14.77	12.81	15.17	13.09	14.89	12.99	14.99	11.63	16.35	12.20	15.78	12.50	15.48	12.94	15.04	13.34	14.64	13.54	14.44
OW-932 L	79.6	78.5	32.79	17.23	15.56	16.01	16.78	15.90	16.89	15.73	17.06	15.35	17.44	15.48	17.31	15.38	17.41	14.14	18.65	14.55	18.24	14.75	18.04	15.27	17.52	15.70	17.09	15.91	16.88
OW-933 L	87.1	86	30.45	14.60	15.85	13.37	17.08	13.29	17.16	13.11	17.34	12.71	17.74	12.84	17.61	12.72	17.73	11.42	19.03	11.85	18.60	12.05	18.40	12.61	17.84	13.07	17.38	13.30	17.15
OW-934 L	100	99	30.94	17.07	13.87	15.83	15.11	15.73	15.21	15.51	15.43	15.09	15.85	15.33	15.61	15.23	15.71	13.78	17.16	14.40	16.54	14.65	16.29	15.23	15.71	15.63	15.31	15.82	15.12

(1) OW-332 L replaced by well OW-332 L (R) in February 2007 prior to the February 2007 monthly water level measurement.
(2) August 2007 readings for OW-408U and OW-420U are questionable due to possible misreading "9" as "6".

RAI 02.04.12-13:

<u>QUESTION</u>:

Please provide the hydrogeologic profiles of all types of wells in the application. Provide typical drawings where appropriate (e.g., relief wells and observation wells). Provide profiles for each production well.

<u>RESPONSE</u>:

Available hydrogeologic profiles and well schematics are provided as follows:

<u>STP Productions Wells</u>:
The location and depths of the STP production wells were established during the subsurface site investigation associated with STP Units 1 & 2. The information is presented in the STP 1 & 2 UFSAR (UFSAR). UFSAR Section 2.5 (Geology and Seismology) provides a description of the geologic conditions beneath the site. The upper 200 feet of the Beaumont Formation (Shallow Aquifer and the Deep Aquifer confining unit) was divided into 13 generalized layers (grouping of major soil types and physical characteristics) presented in UFSAR Section 2.5.4.3 (Exploration Data Gathering Program) and is illustrated in UFSAR Figure 2.5.1-38 (Generalized Stratigraphic Profile). UFSAR Figure 2.5.7-16 (Boring Log No. 114) presents a 750 foot deep boring log from Units 1 & 2, penetrating both the Shallow Aquifer and the Deep Aquifer. The geologic conditions of the Deep Aquifer can be obtained from this boring log.

UFSAR Figure 2.4.13-13 contains a generic well schematic diagram for the production wells installed at STP. A typical pump-test well and piezometer construction schematics for the historical wells installed at STP are also provided as figures in UFSAR Section 2.4.13.

<u>Main Cooling Reservoir (MCR) Relief Wells</u>:
The design and setting of the 7,000-acre MCR are described in FSAR Subsection 2.4S.12.1.5. STP constructed the MCR by building an earthfill embankment above the natural ground surface. The MCR relief well system screen interval depths vary, but are typically 30 feet below ground surface, penetrating the sands of the Upper Shallow Aquifer. The relief wells are installed around the perimeter of the MCR to passively discharge water intercepted from MCR seepage to drainage ditches along the dike toe. The relief wells are designed to be flowing wells whose piezometric heads are higher than the top of the well casing. Attachment (Relief Wells) contains typical relief well design schematics and other information of interest.

<u>STP Historical Piezometers</u>:
The STP 1 & 2 UFSAR describes the historical STP 1 & 2 site-wide piezometers. Figures and Tables of interest include Figure 2.5.C-18 (Location of Permanent Piezometer Installations), Table 2.5.C-2 (Permanent Shallow Aquifer Piezometer Installation Data) and Table 2.5.C-2A (Permanent Deep Aquifer Piezometer Installation Data).

<u>STP Units 3 & 4 Groundwater Observation Wells:</u>
The STP 3 & 4 groundwater observation wells are described in STP 3 & 4 FSAR Section 2.4S.12. FSAR Table 2.4S.12-1 summarizes the observation well construction details. Typical construction logs for two of these wells are provided in Attachment (Observation Wells). A generalized hydrogeologic cross-section is presented in FSAR Figure 2.4S.12-20, which identifies the targeted sand layers at the location of the observation wells.

Simplified well construction logs and the geotechnical boring logs are available from FSAR Reference 2.5S.4-2, the Geotechnical Subsurface Investigation Data Report for STP Units 3 & 4.

References:

1) STP 1 & 2 UFSAR, Revision 13.
2) 2.5S.4-2 "Geotechnical Subsurface Investigation Data Report (Revision 1), Combined Operating License Application (COLA) Project, South Texas Project (STP)," Report by MACTEC Engineering and Consulting, Inc. April 2007.

No COLA revision is required as result of this response.

Attachment (Relief Wells)
STP Units 3 & 4 Typical Relief Wells & Other Information

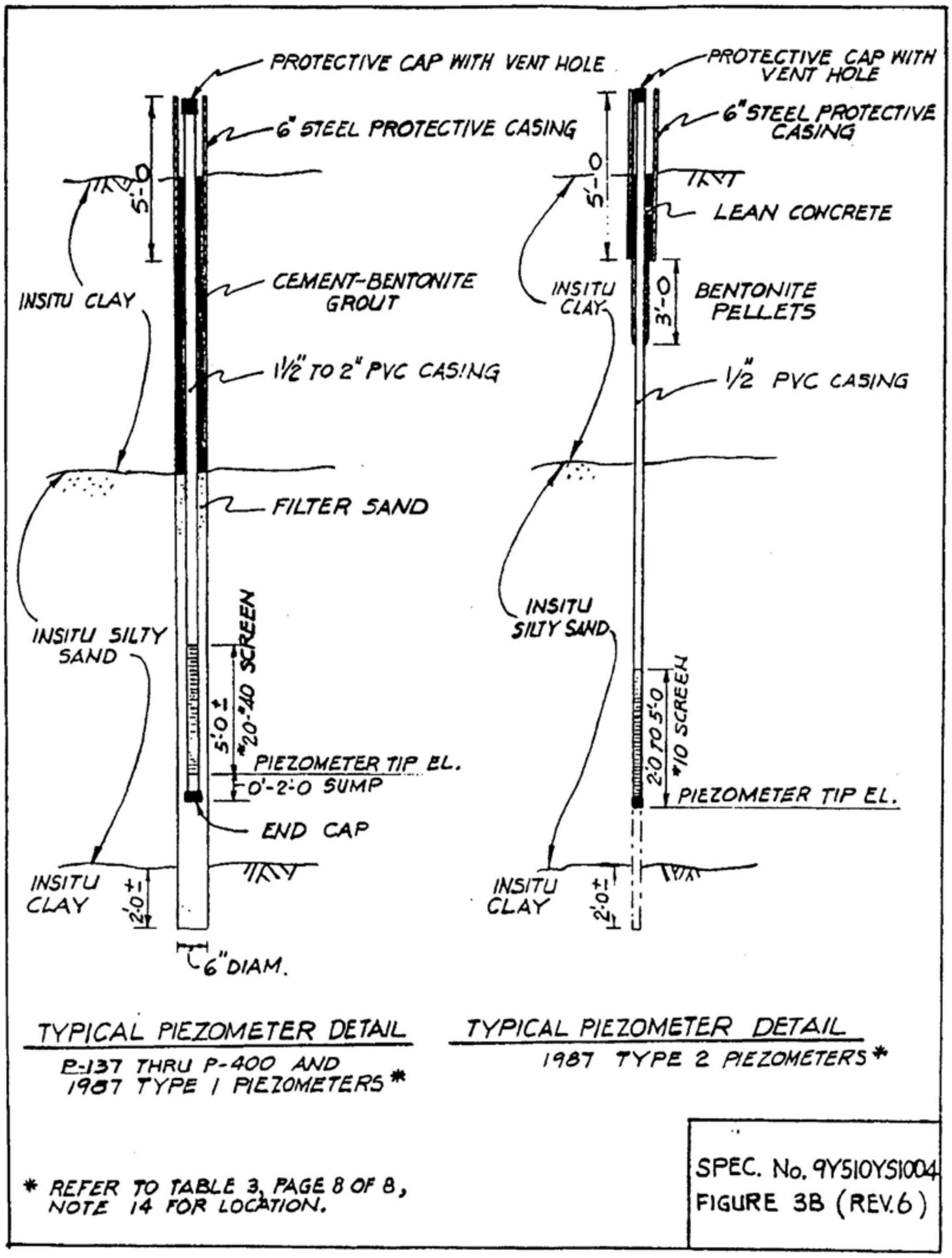
PROTECTIVE CAP WITH VENT HOLE
6" STEEL PROTECTIVE CASING
5'-0
INSITU CLAY
CEMENT-BENTONITE GROUT
1½" TO 2" PVC CASING
FILTER SAND
INSITU SILTY SAND
5'-0 ±
#20-#40 SCREEN
PIEZOMETER TIP EL.
0'-2'-0 SUMP
END CAP
INSITU CLAY
2'-0 ±
6" DIAM.
TYPICAL PIEZOMETER DETAIL
P-137 THRU P-400 AND
1987 TYPE I PIEZOMETERS *
PROTECTIVE CAP WITH VENT HOLE
6" STEEL PROTECTIVE CASING
5'-0
LEAN CONCRETE
INSITU CLAY
3'-0
BENTONITE PELLETS
½" PVC CASING
INSITU SILTY SAND
2'-0 TO 5'-0
#10 SCREEN
PIEZOMETER TIP EL.
INSITU CLAY
2'-0 ±
TYPICAL PIEZOMETER DETAIL
1987 TYPE 2 PIEZOMETERS *
* REFER TO TABLE 3, PAGE 8 OF 8,
NOTE 14 FOR LOCATION.
SPEC. No. 9Y510YS1004
FIGURE 3B (REV.6)

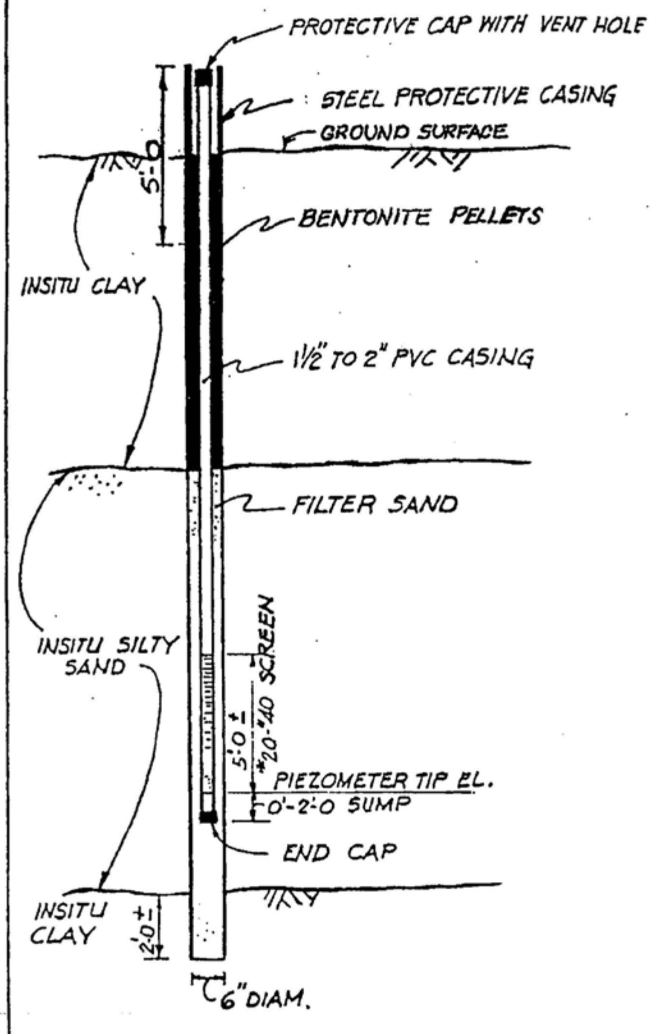

TYPICAL PIEZOMETER DETAIL

P479 THRU P484

1988 PIEZOMETERS

SEE TABLE 3 FOR PIEZOMETER LOCATION.

SPEC. No. 9Y510YS1004
FIGURE 3C (REV. 6)

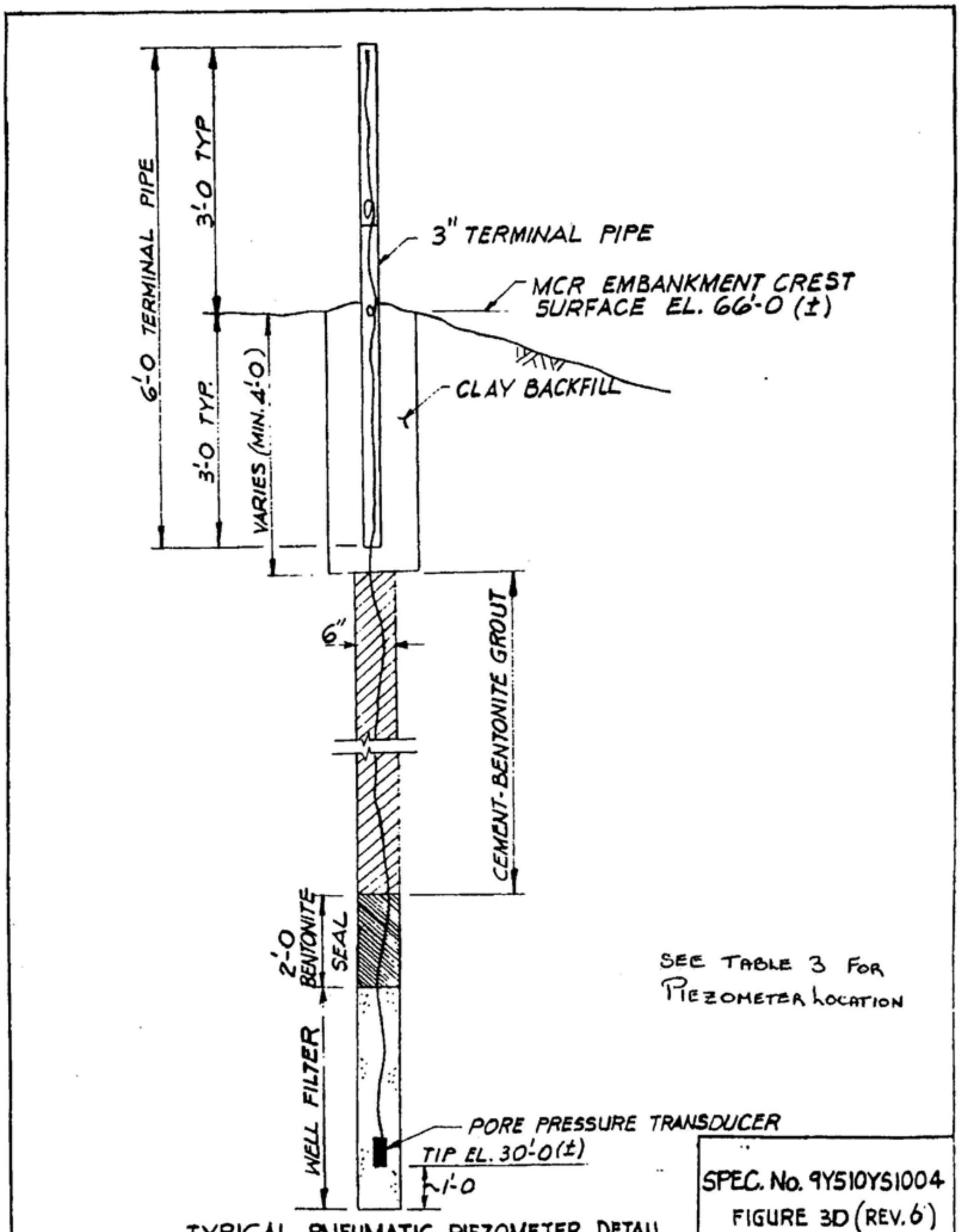

TYPICAL PNEUMATIC PIEZOMETER DETAIL
P454 THRU P470

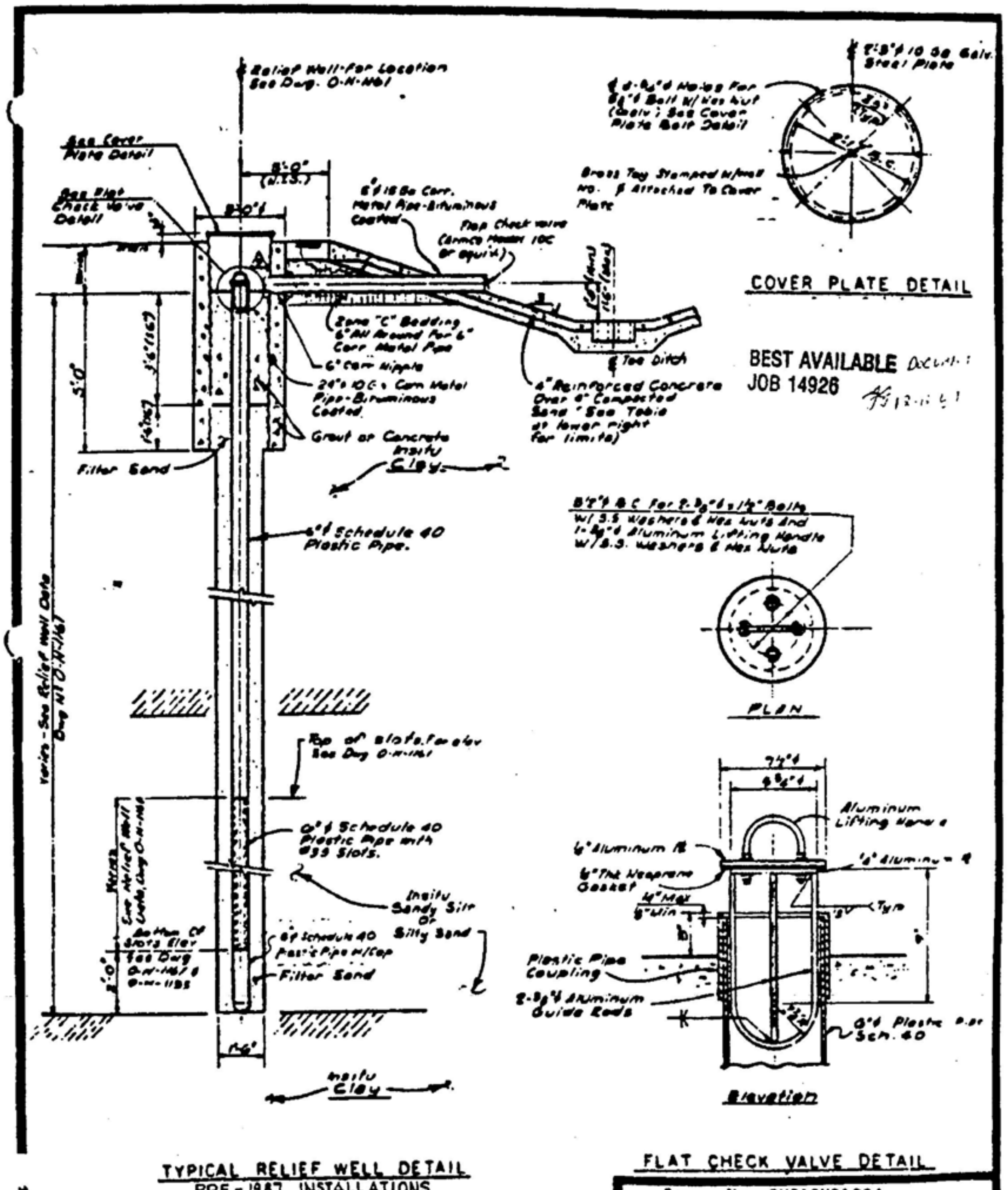

TYPICAL RELIEF WELL DETAIL
PRE-1987 INSTALLATIONS
SEE TABLE 4 FOR RELIEF WELL LOCATION

FLAT CHECK VALVE DETAIL

Spec. No. 9Y510YS1004
Figure 4A(Rev. 6)
Ref. Dwg 0-H-1160

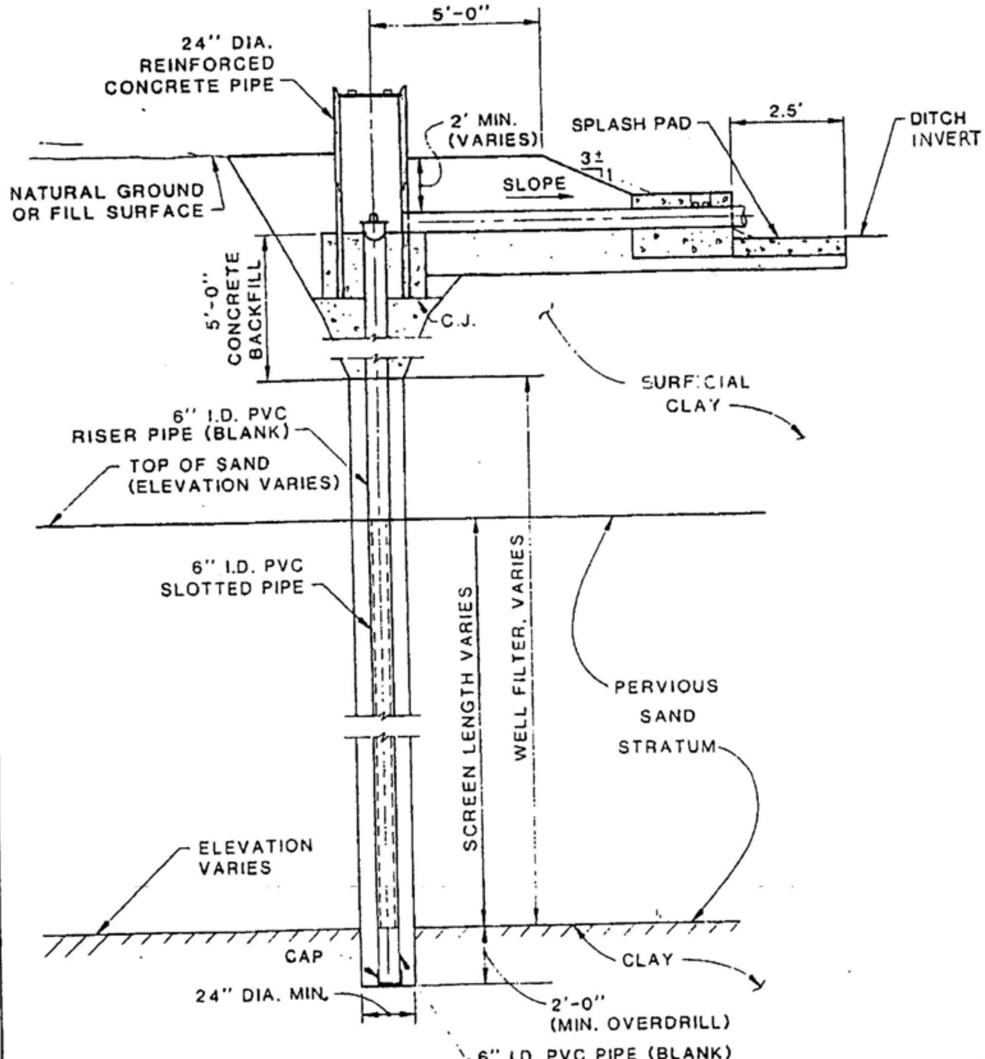

TYPICAL RELIEF WELL
N.T.S.
(WELLS INSTALLED IN 1987)

See Table 4 For Relief Well Location

SPEC. No. 9Y510YS1004
FIGURE 4B (REV.6)
REF. DWG. 1534Q-3-02

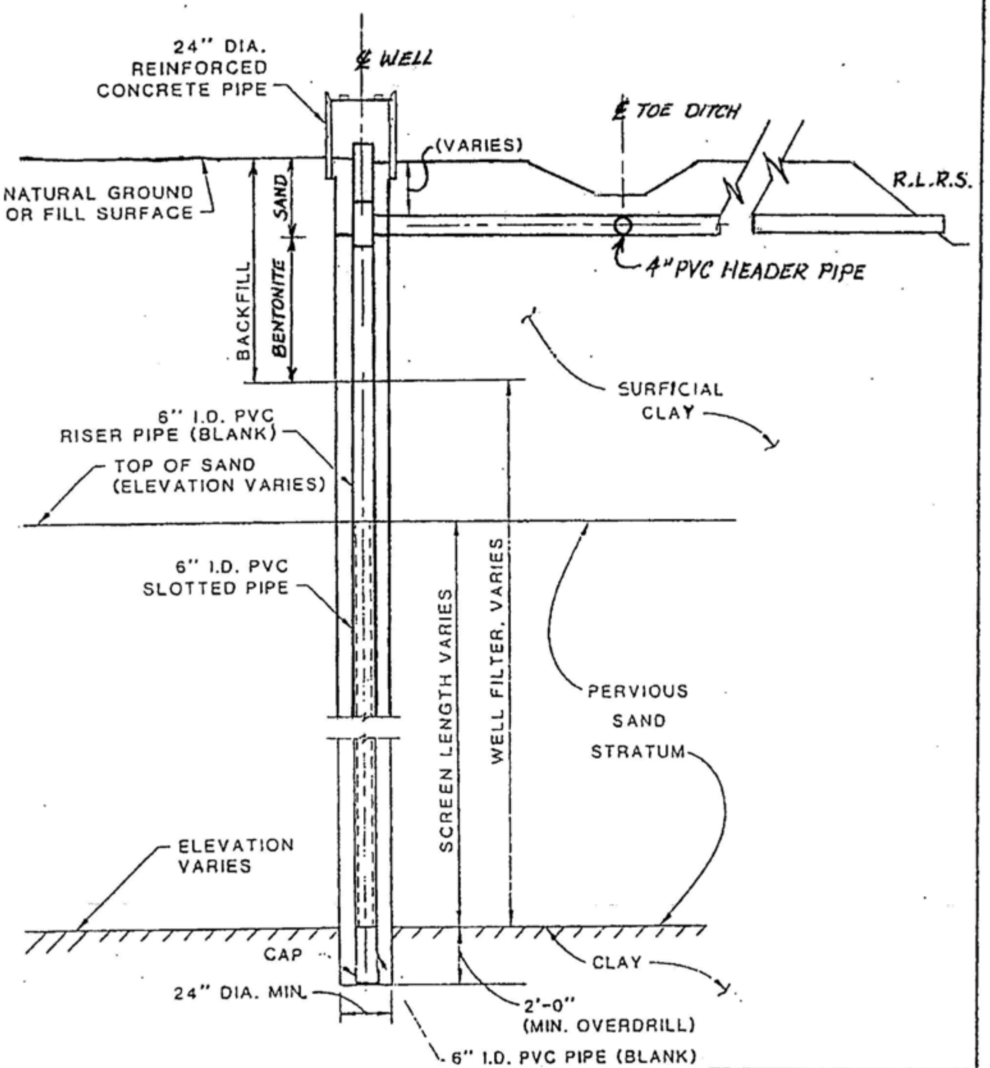

TYPICAL RELIEF WELL
N.T.S.
(WELLS INSTALLED IN 1988)

See Table 4 For Relief Well Location.

SPEC. No. 9Y510YS1004
FIGURE 4c (REV. 6)
REF. DWG. 1534Q-3-02

Attachment (Observation Wells)
STP Units 3 & 4 Typical Observation Well Construction Log Examples

Project Name: STP COL PROJECT Project Number: 6234-08-4632	MACTEC	WELL CONSTRUCTION LOG: OW-308-L
Type of Boring: WASH ROTARY		Boring Location: UNIT 3-REACTOR BUILDING N 363196.43 E 2943374.36
		DATE COMPLETED: 11/22/06

Prepared by MJ Harvey 5-25-08
Checked by KAW 5.28.08

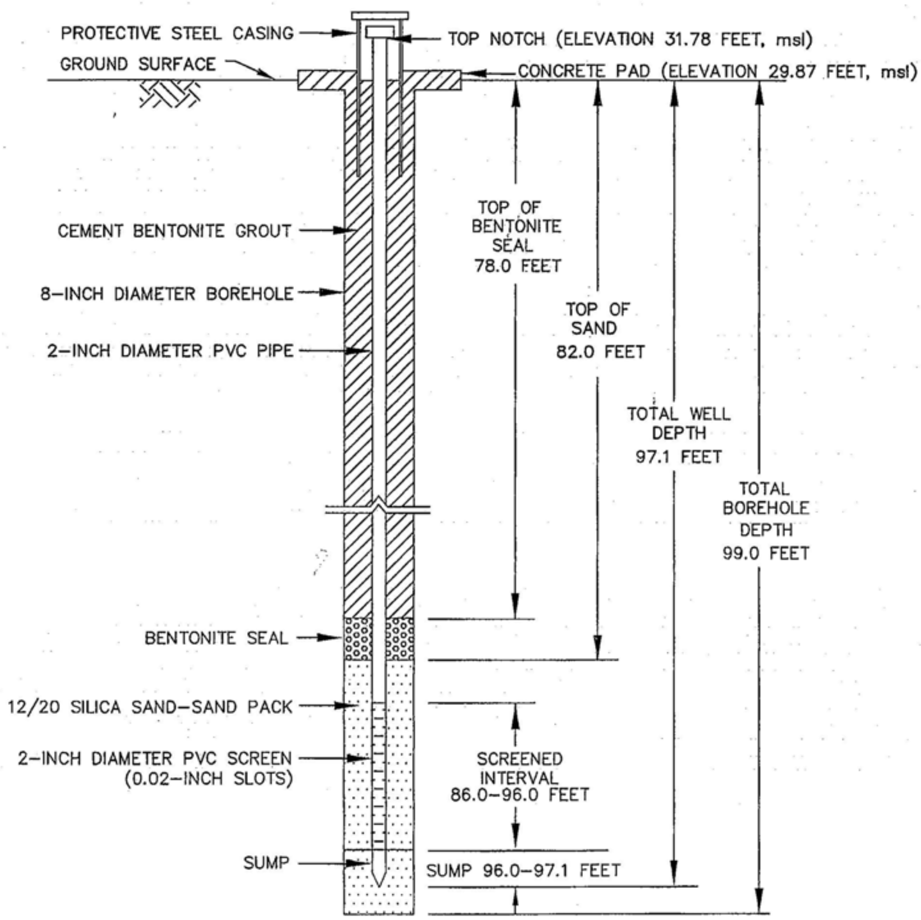

NOTE: 1.) BORING B-308 WAS USED TO DESIGN OW-308-L.
2.) DRAWING NOT TO SCALE.

P:\AutoCAD Drawings Only\Geotechnical\2008\6234-08-4632 STP COL Project\OW.308.L.dwg Thu, 24 Apr 2008 - 8:38am mharriso

Project Name: STP COL PROJECT Project Number: 6234-08-4632	MACTEC	WELL CONSTRUCTION LOG: OW-308-U
Type of Boring: WASH ROTARY		Boring Location: UNIT 3-REACTOR BUILDING N 363195.64 E 2943354.04
		DATE COMPLETED: 11/27/06

Prepared by MJH 5-25-08
Checked by KAW 5.28.08

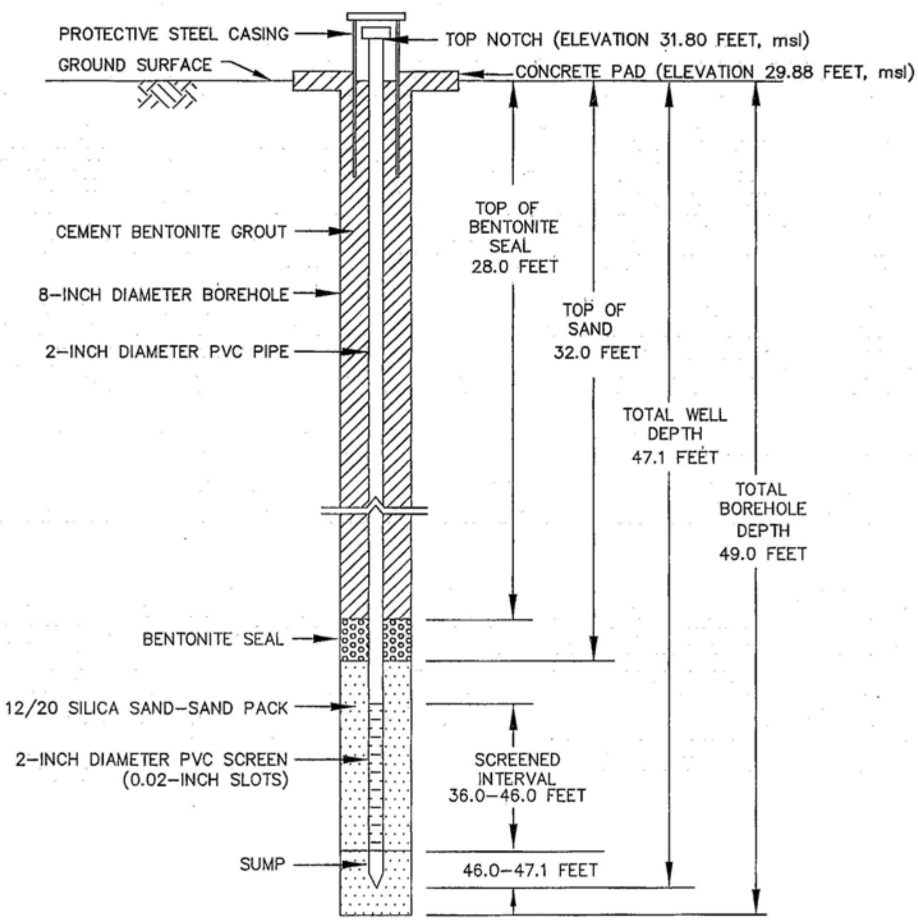

NOTE: 1.) BORING B-308 WAS USED TO DESIGN OW-308-U.
2.) DRAWING NOT TO SCALE.

P:\AutoCAD Drawings Only\Geotechnical\2008\6234-08-4632 STP COL Project\OW.308U.dwg Thu, 24 Apr 2008 - 8:42am mharriso

RAI 02.05.01-11:

QUESTION:

Please explain how a cross section with the orientation of Figure 2.5S.1-47 and with contacts that die out as shown provides evidence for or against displacement on fault I/GMO between boreholes 431 and 432.

RESPONSE:

As described in Subsection 2.5S.1.2.4.2.2.2 of the STP 3 & 4 COLA, the cross section shown in Figure 2.5S.1-47 was constructed from exploratory boring data collected during the geotechnical characterization efforts for STP Units 1 & 2. The cross section was constructed from a series of six borings along what is now the southern embankment of the STP cooling reservoir. The spacing between borings is approximately 2000 to 3000 feet. The original goal of the borings was geotechnical characterization of the subsurface materials; the boring program was not specifically designed or conducted to elucidate shallow stratigraphy at high resolution. As such, the boring logs for the boreholes used in constructing the cross section subdivided subsurface materials into only two types of units (sand and clay) and contain little detail that is useful for identifying and documenting fault offsets (e.g., presence of buried soils in the sediments).

Figure 2.5S.1-45 shows that the surface projection of fault I/GMO as derived from subsurface data (see Subsection 2.5S.1.2.4.2.2.1) crosses the southern embankment of the cooling reservoir at an oblique angle. Given the surface expression of fault I/GMO observed to the west of the cooling reservoir as a zone of distributed tilting (see Subsection 2.5S.1.2.4.2.2.2), offsets of Quaternary deposits beneath the southern cooling reservoir embankment, if present at all, are expected to be characterized by broad monoclinal flexure or folding of the stratigraphy with a vertical offset on the order of several feet over a horizontal distance of hundreds of feet. If such flexure or folding of shallow subsurface materials is present beneath the southern embankment along the cross section of Figure 2.5S.1-47 it would be difficult to detect with the borehole data because:

1) The obliquity of projected surface trace of fault I/GMO to the cross section would increase the apparent horizontal distance over which such an offset would occur (e.g., the apparent slope of the folding or flexure would be significantly decreased from that observed in topographic profiles drawn west of the cooling reservoir (see Subsection 2.5S.1.2.4.2.2.2). This subdued nature of the potential folding would make any subtle folding more difficult to detect.
2) The spacing of the boreholes is large (approximately 2000 to 3000 feet) making it difficult to resolve features (i.e., the potential folding) over shorter or even equivalent lengths.
3) As discussed in Subsection 2.5S.1.2, the site area stratigraphy has considerable variability in the thickness and lateral continuity of sand and clay layers. This variability is due to the fact that fluvial-deltaic depositional environments, like the

one in which the Beaumont Formation was deposited, are not prone to creating laterally extensive deposits of uniform thickness. Without lateral continuity and uniformity in the subsurface sediments, the folding or flexure potentially present from activity of fault I/GMO may be indistinguishable from variations in the site stratigraphy caused by the depositional environment.

The cross section shown in Figure 2.5S.1-47 does not provide evidence for or against the absence of folding or flexure beneath the southern embankment of the cooling reservoir between boreholes 431 and 432 related to activity of fault I/GMO.

No COLA Revision is required as a result of this response.

RAI 02.05.01-16:

<u>QUESTION</u>:

Please explain the units marked as “Bay City,” “El Campo,” and “Lolita” in Figure 2.5S.1-14. What are their origin and age and what are their relevance to the site? Are these units consistent with current ideas on sediments and landforms of this age in Blum and Aslan (2006) and references therein?

<u>RESPONSE</u>:

Figure 2.5S1-14 shows the location of the STP 3 & 4 site relative to informal subdivisions of the Beaumont Formation (Bay City, El Campo, and Lolita) as mapped by Blum and Price (1998) and Blum and Aslan (2006). The Beaumont Formation within the STP 3 & 4 site vicinity is composed of sediments deposited during interglacial transgression-regression sequences as facies of alluvial fan-delta systems within the Colorado and Brazos fluvial systems. The subdivisions of the Bay City, El Campo, and Lolita identified by Blum and Aslan (2006), Aslan and Blum (1999), and Blum and Price (1998) are based on the identification of three distinct valley fills within Beaumont Formation deposits; each valley fill corresponds to one of the unit subdivisions. The subdivisions are designated by their geomorphic expressions and the unique paleosols associated with each valley fill.

Historically the Beaumont Formation has been interpreted as being deposited between 150,000 and 100,000 years ago (Barnes, 1987; Dubar et al., 1991; Winker, 1979). However, with the identification of the three distinct Beaumont valley fill deposits, researchers also noted that deposition of the Beaumont Formation occurred over a much longer period of time. This longer period of deposition is recorded in the age of the valley fill sediments. Thermoluminescence (TL) dating on the valley fills indicate that the Lolita valley fill was deposited approximately 350,000 years ago during the interglacial period associated with marine Oxygen Isotope Stage (OIS) 9 based on TL ages of 323,000 ± 51,000 and 307,000 ± 37,000 years ago (Blum and Price, 1998). TL ages from the Bay City valley fill (119,000 ± 10,000; 119,000 ± 9,000; 115,000 ± 7,000; 102,000 ± 6,000; 155,000 ± 15,000; and 96,400 ± 6200 years ago) indicate deposition occurred during OIS 6 to 5 from approximately 150,000 to 100,000 years ago (Blum and Price, 1998; Blum and Aslan, 2006). The El Campo valley fill has not been dated but lies stratigraphically between the Lolita and Bay City indicating that the age of its deposition is intermediate to that of the Lolita and Bay City. These subdivisions of the Beaumont Formation are consistent with the current interpretation of the depositional environment of the Beaumont Formation as outlined in Blum and Aslan (2006) and references cited therein.

As mapped by Blum and Aslan (2006) the STP 3 & 4 site lies within the Bay City valley fill of the Beaumont Formation. This valley fill is composed of highly heterogeneous sands, silts, clays and estuarine muds typical of the fluvial-deltaic deposits of the Beaumont Formation. The particular significance of these valley fills relative to the STP 3 & 4 site is that the site lies on the youngest valley fill that was deposited between approximately 100,000 to 150,000 years ago.

No COLA Revision is required as a result of this response.

References:

Aslan, A., and Blum, D., 1999, Contrasting styles of Holocene avulsion, Texas Gulf Coastal Plain, USA: Special Publications of the International Association of Sedimentologists, v. 28, p. 193-209.

Barnes, V.E., 1987, Geologic Atlas of Texas Beeville-Bay City Sheet: Austin, TX, Bureau of Economic Geology.

Blum, M., and Price, D.M., 1998, Quaternary alluvial plain construction in response to glacio-eustatic and climatic controls, Texas Gulf coastal plain, Relative Role of Eustacy, Climate, and Tectonism in Continental Rocks, Society for Sedimentary Geology, Special Publication 59, p. 31-48.

Blum, M.D., and Aslan, A., 2006, Signatures of climate vs. sea-level change within incised valley-fill successions: Quaternary examples from the Texas Gulf Coast: Sedimentary Geology, v. 190, p. 177-211.

Dubar, J.R., Ewing, T., Lundelius, E.L., Otvos, E.G., and Winker, C.D., 1991, Quaternary Geology of the Gulf of Mexico Coastal Plain, in Morrison, R.B., ed., Quaternary Nonglacial Geology: Conterminous U.S., Volume K-2: Boulder, CA, Geological Society of America, Geology of North America, p. 583-610.

Winker, C.D., 1979, Late Pleistocene Fluvial-Deltaic Deposition: Texas Coastal Plain and Shelf [MA thesis]: Austin, TX, University of Texas at Austin.

RAI 02.05.02-1:

QUESTION:

Equation 2.5S.2-3 shows how magnitude uncertainty, sigma(mb), was used to compute uniform, unbiased magnitudes. Section 2.5S.2.1.2 states that sigma(mb) was estimated for each earthquake in the updated catalog, but does not describe how sigma(mb) was estimated. Please explain the method used to estimate sigma(mb).

RESPONSE:

Equation (4-2) of Reference 2.5S.2-3 indicates the equation from which m_b* (or Rmb) is estimated from the best estimate of magnitude $E[m_b]$ (or Emb) and the uncertainty in mb, sigma(mb) (or σ_{mb} or Smb), when mb is determined through conversion from other size measures:

$$m_b^* = E[m_b] + (1/2)\cdot\ln(10)\cdot b\cdot\sigma_{mb}^2$$

where the variance, σ_{mb}^2 (or sigma(mb)^2) and a single value of $b = 1.0$ have been used to calculate m_b*.

Reference 2.5S.2-3 does not explicitly describe how sigma(mb) was determined. However, an examination of the EPRI catalog, particularly sigma(mb) values listed and the various size measures from which they were determined, shows that this value can be estimated from the different earthquake size estimates available for a given event. By inspection of the Reference 2.5S.2-3 catalog, the following appears to be a correlation of sigma(mb) and the available earthquake size estimates:

Size measure	Sigma(mb)
body wave magnitude [Mb, MB, mb, MN, Mn, Lg]	0.10
coda (or duration) magnitude [MD, Md, md, mc] + intensity + felt area	0.22
coda (or duration) magnitude [MD, Md, md, mc] and local magnitude [ML, mL]	0.23
coda (or duration) magnitude [MD, Md, md, mc] + intensity	0.27
coda (or duration) magnitude only [MD, Md, md, Mc, mc]	0.30
local magnitude [ML, mL] + intensity	0.33
local magnitude [ML, mL] only	0.41
Surface wave magnitude [MS, Ms]	0.41
intensity only	0.56

These values of sigma(mb) were used to update the EPRI (1988) earthquake catalog in analogy with the original catalog.

No COLA revision is required as a result of this RAI response.

References:

2.5S.2-3 "Seismic Hazard Methodology for the Central and Eastern United States," Volume 1, Part 2: Methodology (Revision 1), EPRI NP-4726-A, Rev. 1, Electric Power Research Institute (EPRI), November 1988.

RAI 02.05.02-2:

QUESTION:

The original EPRI/SOG report (Reference 2.5S.2-3) recommends Equation 4-2 (FSAR Equation 2.5S.2-3) for computing uniform magnitudes "when mb is determined through conversion from other size measures," but a different equation, Equation 4-3 in the original EPRI/SOG report, when mb "is determined directly from instrumental data" – presumably the case for most of the updated catalog. Please explain why you used Equation 4-2 to compute uniform magnitudes for the post-1984 earthquakes instead of Equation 4-3.

RESPONSE:

Reference 2.5S.2-3 presents two equations for conversion of $E[m_b]$ to mb* (or Rmb):

(Reference 2.5S.2-3, Eqn. 4.2) $m_b^* = E[m_b] + (1/2)\cdot\ln(10)\cdot b\cdot\sigma_{mb}^2$
(Reference 2.5S.2-3, Eqn. 4.3) $m_b^* = E[m_b] - (1/2)\cdot\ln(10)\cdot b\cdot\sigma_{mb}^2$

and specifies that the first is to be used "when mb is determined through conversion from other size measures" and the second when "$E[m_b]$ is determined directly from instrumental data and reflects uncertainty of this direct estimation." Reference 2.5S.2-3 further states that when $E[m_b]$ is determined directly from instrumental data the variance is small so that the instrumental value can be used with little error. In fact, inspection of EPRI's final seismicity catalog shows that the first equation (4.2) was applied to calculate m_b^* in all cases for both mb converted from other size measures as well as for cases where mb had presumably been determined directly from instrumental data. To be consistent with the methodology ultimately used to develop the original EPRI catalog, and to avoid introducing unnecessary complexity into the catalog update, equation (4.2) was used to determine m_b^*'s in all cases.

No COLA revision is required as a result of this RAI response.

References:

2.5S.2-3 "Seismic Hazard Methodology for the Central and Eastern United States," Volume 1, Part 2: Methodology (Revision 1), EPRI NP-4726-A, Rev. 1, Electric Power Research Institute (EPRI), November 1988.

RAI 02.05.02-3:

<u>QUESTION</u>:

In Section 2.5S.2.1.3, you used Equation 2.5S.2-4 to convert Ms to mb for the Gulf of Mexico earthquakes. Please provide a reference for the equation, and explain why you used a different approach to convert Ms to mb for the post-1984 catalog (Ms to M to mb, as described in Section 2.5S.2.1.2).

<u>RESPONSE</u>:

The reference for Equation 2.5S.2-4 is Equation 4-1 of Reference 2.5S.2-3. Parameters utilized are contained in Table 4-1 of EPRI 1988 (Reference 2.5S.2-3).

The earthquake catalog presented in FSAR Section 2.5S.2 was developed in two phases. In the first phase, 2.5S.2.1.2, the EPRI-SOG catalog was taken as complete through 1984 and the EPRI-SOG catalog was updated in the large geographic window of 107° W to 83° W, 24° N to 40° N for events occurring after 1984. This geographic window incorporates the seismic sources contributing significantly to the STP 3 & 4 site earthquake hazard.

As discussed in FSAR Section 2.5S.2.1.3, subsequent to the initial phase of updating the seismicity catalog, it was assessed that a portion of the Gulf of Mexico might not have been fully covered by the pre-1985 EPRI-SOG seismicity catalog. This was suggested by the southern boundary of the area for which probability of detection matrices were developed for the EPRI-SOG study (see FSAR Figure 2.5S.2-7). A second phase of seismicity catalog update, therefore, was conducted over <u>all</u> time in the southeast corner of the seismicity catalog investigation region: 100° W to 83° W, 24° N to 32° N, referred to as the Gulf of Mexico Investigation Region.

During the first phase of seismicity update, there were two events [December 31, 2002, Ms 3.50; February 10, 2006, Ms 5.20] found with surface wave magnitudes [Ms] that were converted to a best estimate of body wave magnitude [Emb] using: 1) Figure 6 of Reference 2.5S.2-14 to convert from Ms to moment magnitude [**M**], and, 2) FSAR Table 2.5S.2-1 to convert from **M** to mb. This conversion resulted in Emb values of 4.66 and 5.87 for the 2002 and 2006 events, respectively.

During the second phase of the seismicity catalog update, it was determined that there was an EPRI-SOG equation [FSAR Equation 2.5S.2-4] to convert Ms to Emb directly. For updating the seismicity catalog, there was a methodological preference to be consistent with EPRI-SOG methodologies wherever reasonable. Therefore, it was intended that the two Ms magnitudes be re-converted to mb using Equation 2.5S.2-4. The 2006 event, located within the Gulf of Mexico Investigation Region, was re-converted to mb 5.52. Because it lies outside the Gulf of Mexico, the 2002 event Ms magnitude was not re-converted. The re-conversion of the 2002 Ms magnitude would have resulted in an mb 4.47, instead of mb 4.66, as given in the FSAR. This difference in these converted magnitudes for the 2002 event has no significant effect on the evaluation of vibratory ground motion for the site.

COLA Section 2.5S.2.1.3 [near the end of this section] will be revised as follows:

In the development of the revised composite project seismicity catalog, the magnitudes given in all catalogs were converted to best, or expected, estimates of *mb* (Emb), using the same conversion equations discussed above with the following additions:

Surface wave magnitudes [Ms] given in the catalogs were converted to EPRI best, or expected, estimates of body wave magnitude (E[mb], also referred to as Emb in Reference 2.5S.2-3) using the conversion factors given as equation 4-1 and Table 4-1 in Reference 2.5S.2-3:

$$\text{Emb} = 2.302 + 0.618 \cdot \text{Ms} \qquad \text{Equation 2.5S.2-4}$$

where Ms is surface wave magnitude.

References:

2.5S.2-3 "Seismic Hazard Methodology for the Central and Eastern United States," Volume 1, Part 2: Methodology (Revision 1), EPRI NP-4726-A, Rev. 1, Electric Power Research Institute (EPRI), November 1988.

2.5S.2-14 "Estimating Ground Motions Using Recorded Accelerograms," Surveys in Geophysics, v. 8, pp. 25-83, Heaton, T.H., F. Tajima, and A. W. Mori, 1986.

RAI 02.05.02-4:

QUESTION:

Please explain why you applied different declustering criteria to the two parts of the updated seismic catalog (Gulf of Mexico and post EPRI SOG for the rest of the study area). Please describe the approach or algorithm used to decluster the updated Gulf of Mexico catalog, and explain what is meant by "guided by the EPRI characterization of MAIN vs. non-MAIN, as well as by apparent spatial and temporal similarity between events, dependent events were identified and removed" (FSAR Section 2.5S.2.1.3).

RESPONSE:

As discussed in FSAR Section 2.5S.2.1, as well as the response to RAI 02.05.02-3, the development of the updated seismicity catalog occurred in two phases. The first phase was to update the EPRI-SOG seismicity catalog for the entire project investigation region – 24°N to 40°N, 107°W to 83°W – from 1985 to current. Upon recognition that the EPRI-SOG seismicity catalog [covering a time period through 1984] may not have been complete in the Gulf of Mexico, a second phase of update that looked at seismicity for all time was undertaken for the Gulf of Mexico.

For the first phase, there were no known notable clusterings of seismicity near to the site, similar to the 1964 Hemphill, Texas series, so no concerted effort was made to remove possible dependent events [i.e., aftershocks, foreshocks, series clusters]. While it is recognized that some dependent events may yet be in the 1985 to current update, it allows for a possible conservative [i.e., higher], though not excessive, assessment of post-EPRI-SOG seismicity rate, which, if proved significant relative to the 1988 EPRI-SOG seismicity rates (Reference 2.5S.2-3), would have warranted closer scrutiny on the catalog for any possible dependent events.

In the development of the updated seismicity catalog for the project site, the southeastern portion of the project catalog investigation window – referred to here as the Gulf of Mexico [GoM] investigation region, 24°N to 32°N, 100°W to 83°W – was given closer scrutiny, as discussed in Section 2.5S.2.1.3. Because recurrence parameters would have to be developed for empty 1° by 1° cells of some EPRI-SOG source zones in the Gulf of Mexico, closer evaluation was made of dependent [i.e., aftershock, foreshock, series cluster] events. As is apparent in Figure 2.5S.2-7, at least the northern portion of this GoM region was covered by the EPRI-SOG seismicity catalog. In the process of looking at seismicity for <u>all time</u> in the GoM region, the dependent EPRI-SOG catalog events, identified as non-MAIN, were initially retained in the compilation with nine other earthquake catalogs considered [see FSAR Section 2.5S.2.1.3]. A simple program was used to identify duplicates: specifically, any events coming from different source catalogs are assumed duplicates if they have origin times within 60 seconds. [Note: this process may not identify actual additional duplicates for older events, where the event timing is not as precise or accurate. See below.] In the process of identifying duplicate events among the ten catalogs, the EPRI-SOG catalog [MAIN and non-MAIN] was given the highest priority. Therefore, any events introduced from the other nine catalogs and determined to be duplicates of a non-MAIN EPRI event were themselves identified as dependent events. Subsequently, the preferred non-MAIN EPRI events were removed from the final catalog – since only independent events are desired in the final catalog wherein probabilistic seismic hazard analysis (PSHA) earthquake statistics are of interest – eliminating the associated identified dependent duplicates from the other nine catalogs. This is the process of removing dependent events – commonly referred to as *declustering* – among the nine non-EPRI catalogs by their association to non-MAIN EPRI events, implied in the phrase "guided by the EPRI characterization of MAIN vs. non-MAIN".

The resulting GoM investigation region catalog was then manually reviewed – no computer code was used – to further identify possible dependent events or those that appeared to be duplicates that were not identified as such within the tight time window [60 seconds] used to programmatically identify duplicates, as discussed above. There are cases – particularly earlier historical records, where the 60-second time window is too small. A manual review of the catalog can identify these as duplicates based on similarity of time and location. For example:

```
         1         2         3         4         5         6         7         8         9         0         1
....5....0....5....0....5....0....5....0....5....0....5....0....5....0....5....0....5....0....5....0....5....0....5.

CAT       D  A  T  E    C **COORDINATES**     D  STN.****** M A G N I T U D E S ******FE#   ** INFORMATION * RADIAL
SRCE YYYYYYMMDDHHMMSS.SSO   LAT      LONG DEP  C  DEV.      Ms Z##                          S#Q          PHENOM.  DIST.
                        T   +N        +E  km   D      mb ##   /  Mag1ScDonorMag2ScDonor      IEMFMDIPF          km
                        A +xx.xxx        iii   pP            H      al          al           NFAPOEDFL
                        aa       +xxx.xxx             x.x  x.x   x.xx e     x.xx e           TFPS PEDG


SRA   1873  5 1 0 0 0.00Z  30.200 -97.700  0         0.0 00.0  00.00       0.00       500G 3..............       .0  .00

EPRI  1873  5 1 430 0.00   30.200 -97.700  0         3.6 00.0  02.81mbEPRIe3.17mbEPRIr  0  4                   221.4 2.81mbEPRIe MAIN
    DPC         430 0.00   30.250 -97.600  0         0.0 00.0  03.10       0.00         0  .                       .0  .00
    SRA         430 0.00Z  30.250 -97.600  0         0.0 00.0  03.60FASRA  0.00       500G 4..............       .0  .00
```

The EPRI event at 5/1/1873 at 4:30 is preferred over two duplicates [programmatically identified and indented] within the 60-second window coming from the DPC and SRA catalogs. An "earlier" event from the SRA catalog on the same day, but no time given, may be a duplicate or an earlier separate, but dependent event [same day, very near same location] of the larger one given at the specific time of 4:30. This earlier event was assessed to be a duplicate or dependent event and manually removed from the compiled catalog.

Obviously related events were scrutinized for dependence. A clear example is given from the 1964 Hemphill, Texas earthquake sequence. The main event was identified in EPRI. Also shown here are EPRI non-MAIN events [indicated by the '*' at the end], but also annotation on duplicates [indented] and dependent events that were identified and removed from the final catalog.

```
         1         2         3         4         5         6         7         8         9         0         1
....5....0....5....0....5....0....5....0....5....0....5....0....5....0....5....0....5....0....5....0....5....0....5.

CAT       D  A  T  E    C **COORDINATES**     D  STN.****** M A G N I T U D E S ******FE#   ** INFORMATION * RADIAL
SRCE YYYYYYMMDDHHMMSS.SSO   LAT      LONG DEP  C  DEV.      Ms Z##                          S#Q          PHENOM.  DIST.
                        T   +N        +E  km   D      mb ##   /  Mag1ScDonorMag2ScDonor      IEMFMDIPF          km
                        A +xx.xxx        iii   pP            H      al          al           NFAPOEDFL
                        aa       +xxx.xxx             x.x  x.x   x.xx e     x.xx e           TFPS PEDG

EPRIm 1964   424 73351.90   31.420 -93.810  5         0.0 00.0  03.58mbEPRIe3.59mbEPRIr  0   4                  360.5 3.58mbEPRIe
    ANSS         73353.00   31.600 -93.800 33         0.0 00.0  03.70MbNEI  0.00         0  0.                      .0  .00
    ISC          73352.30   31.510 -93.860 33         0.0 00.0  03.60mbISC  0.00         0  0..   ...........       .0  .00
    SRA          73351.90   31.422 -93.812  5         3.7 00.0  03.60MnSRA  0.00       504A  5..............       .0  .00

EPRI  1964   424 74717.10   31.380 -93.800  5         0.0 00.0  03.28mbEPRIe3.29mbEPRIr  0  .                   357.6 3.28mbEPRIe*
```

```
    SRA         74717.10   31.384 -93.804  5         0.0 00.0  03.20MnSRA  0.00       504B ................       .0  .00
>>> Remove as non-MAIN event

SRA   1964  424 75056.00   31.300 -93.800  0         0.0 00.0  02.60MnSRA  0.00       504C ................       .0  .00
>>> Assumed cluster event with EPRI MAIN - Remove
>>> not in EPRI catalog

EPRI  1964  42412 7 8.20   31.480 -93.790  9         3.2 00.0  03.18mbEPRIe3.19mbEPRIr  0  .                  367.0 3.18mbEPRIe*
    SRA        12 7 8.20   31.478 -93.787  9         0.0 00.0  03.20MnSRA  0.00       504C 4...............       .0  .00
>>> Remove as non-MAIN event

EPRI  1964  424125417.00   31.300 -93.800  0         3.0 00.0  02.98mbEPRIe2.99mbEPRIr  0  .                  350.7 2.98mbEPRIe*
    SRA       125417.00   31.300 -93.800  0         0.0 00.0  02.90MnSRA  0.00       504C ................       .0  .00
>>> Remove as non-MAIN event

SRA   1964  424172213.00   31.300 -93.800  0         0.0 00.0  02.80MnSRA  0.00       504C ................       .0  .00
>>> Assumed cluster event with EPRI MAIN - Remove

SRA   1964  42423 350.00   31.300 -93.800  0         0.0 00.0  02.60MnSRA  0.00       504C ................       .0  .00
>>> Assumed cluster event with EPRI MAIN - Remove
>>> not in EPRI catalog
```

Again, it is recognized that some otherwise interpreted dependent events may yet remain in the Gulf of Mexico investigation region, but the process followed here would be expected to identify most dependent events that could affect recurrence parameter evaluation of the required EPRI-SOG source cells.

No COLA revision is required as a result of this RAI response.

References:

2.5S.2-3 "Seismic Hazard Methodology for the Central and Eastern United States," Volume 1, Part 2: Methodology (Revision 1), EPRI NP-4726-A, Rev. 1, Electric Power Research Institute (EPRI), November 1988.

RAI 02.05.02-6:

QUESTION:

In Section 2.5S.2.1.5, you developed a new earthquake-detection probability matrix and catalog-completeness model for the Gulf of Mexico region. You based its analysis on the assumption that earthquake detection probabilities for a given magnitude increase with time. Please explain how you can confirm that local and regional seismograph coverage in the study region was experiencing improvement or was at least stable during the time period of the analysis?

RESPONSE:

The matrix of detection probabilities developed for the Gulf of Mexico needed to cover the potential time period of coverage of the complete catalog, so it was developed to extend from as early as 1625 [same starting time as the EPRI seismicity characterization] to the present. The two major factors in detection of an earthquake are demographics – that is, the presence of people available to possibly record the effects of an earthquake – and the distribution of seismographic instrumentation, locally, regionally, and globally, to record earthquakes. Over time, populations have generally grown, and the distribution of seismographic stations has also improved. Therefore, there is generally a presumption of improvement of detection capability with time. Detection probabilities, of course, cannot exceed 1.0.

In developing the matrix for the Gulf, there is an obvious lack of local and regional population and seismographic station coverage so that probabilities of detection are reasonably expected to be less than those associated with the nearest onshore matrices, presented in Reference 2.5S.2-3.

The trends discussed above, as well as additional constraints discussed in the FSAR, were used to develop the Gulf of Mexico matrix.

This follows the assumptions used in Reference 2.5S.2-3 to develop the original probability of detection functions for all completeness regions, and our intent was always to extend Reference 2.5S.2-3 parameters following the EPRI methodology as closely as possible.

No COLA revision is required as a result of this RAI response.

References:

2.5S.2-3 "Seismic Hazard Methodology for the Central and Eastern United States," Volume 1, Part 2: Methodology (Revision 1), EPRI NP-4726-A, Rev. 1, Electric Power Research Institute (EPRI), November 1988.

RAI 02.05.02-7:

QUESTION:

In section 2.5S.2.1.5, you assumed that the seismic activity of two regions (the Gulf of Mexico and CEUS) are similar by replacing the calculated b value of 0.5 from the Gulf of Mexico seismic catalog with the b value 1.0 from the CEUS. What is the basis for this assumption?

RESPONSE:

The "b" value implied by the seismicity of the Gulf of Mexico and our assumptions about the probability of detection of earthquakes in the Gulf for magnitude-time cells of the probability of detection matrix was used as a final check on the reasonableness of the matrix. Initial assumptions about the probability of detection of several cells, in particular those giving the probability of detection of larger earthquakes (magnitude 5.7 to 6.29 and 6.3 to 7.5) for earlier time intervals (1900 to 1924 and 1925 to 1949) (the highlighted cells in Table 2.5S.2-6 of the FSAR) were found to result in "b" values lower than typical globally or for stable continental interiors (0.8 to 1.2, see Reference 2.5S.2-25, Table 2; Reference 2.5S.2-26, Table 4-7 for stable continental regions), lower than those assumed by Reference 2.5S.2-3 in the development of uniform magnitude estimates, and lower than those assumed by the Earth Science Teams participating in the EPRI-SOG study (see Tables 2.5S.2-7 through 2.5S.2-11 of the FSAR).

As a final step in the development of the probability of detection matrix, the values in the highlighted cells were modified in a way judged to be reasonable, yet resulting in a global "b" value for the Gulf seismicity more in line with regional expectations. That is, using the detection probability matrix of Table 2.5S.2-6 with the seismicity of the Gulf of Mexico, a maximum likelihood "b" value of 1.055 was obtained, allowing the conclusion that the matrix of detection probability presented in Table 2.5S.2-6 is a reasonable characterization of the completeness of the seismicity in the Gulf of Mexico.

It is important to note that the "b" value attributed to any degree-by-degree subarea of any Gulf of Mexico earthquake source model of any Earth Science Team depends principally on the areal and size distribution of Gulf seismicity, on the smoothing assumptions made by the ESTs on seismic activity rate, and on any priors and the strength of any priors placed on "b" within these model sources by the ESTs. The analysis of "a" and "b" for each cell in the development of the site-specific probabilistic seismic hazard analysis (PSHA) does not directly use the "b" values [i.e., 0.5 or 1.055], discussed in this FSAR section on the development of the probability of detection matrix, which only secondarily affects the analysis in the manner in which these test "b" values were used to guide the development of the matrix.

No COLA revision is required as a result of this RAI response.

References:

2.5S.2-3 "Seismic Hazard Methodology for the Central and Eastern United States," Volume 1, Part 2: Methodology (Revision 1), EPRI NP-4726-A, Rev. 1, Electric Power Research Institute (EPRI), November 1988.

2.5S.2-25 "Chapter 41: Global Seismicity: 1900 – 1999," International Handbook of Earthquake & Engineering Seismology, pp. 665 – 690, Engdahl, E.R. and Villaseñor, A., 2002.

2.5S.2-26 "The Earthquakes of Stable Continental Regions," Volume 1: Assessment of Large earthquake Potential, EPRI Final Report TR-102261-V1, Johnston, A.C., K.J. Coppersmith, L.R. Kanter, and C.A. Cornell, Electric Power Research Institute (EPRI), December 1994.

RAI 02.05.04-5:

<u>QUESTION</u>:

Tables 2.5S.4-34 and 2.5S.4-35 list points of potential liquefaction within layers determined by the SPT and CPT. Tier 1 of the DCD does not allow liquefaction to occur at the plant site. Please provide a graphic interpretation of the areal extent in plan and profile of the liquefiable zones based on SPT and CPT and justify the occurrence of liquefaction with respect to the DCD Tier 1 requirement.

<u>RESPONSE</u>:

The UHS design described in Revision 1 of the STP 3 & 4 COLA is being modified. The following RAI response applies to the UHS design as currently described in COLA Revision 1. This response will be updated, if necessary, following completion of the UHS design modification, which will be presented in the next revision of the COLA.

DCD/Tier 1, Table 5.0, "ABWR Site Parameters" says, "Liquefaction Potential: none at plant site resulting from site specific SSE ground motion." This statement refers to the plant site after plant construction when liquefiable soil has been removed or improved so that it is no longer liquefiable.

SPT Results

Table 2.5S.4-34 and Subsection 2.5S.4.8.2.2 summarize the results of liquefaction analyses using SPT results and tabulate boring locations and depths where the computed Factor of Safety (FOS) against liquefaction is < 1.1. The section states that 15 out of the 3,389 SPT results analyzed showed FOS < 1.1. The results reported in the table under the heading "Stratum (Disposition)" additionally take into account the soil type, the depth of the sample, and whether the soil will be excavated out during construction.

7 of the 15 samples were from areas to be excavated.

Of the remaining 8 results, 2 were from clay soils (layers D and N (Clay)) which are very unlikely to liquefy.

Of the 6 remaining results:

- The sample at El -348.7 ft under the Unit 3 reactor building has FOS = 1.03. The age (Pleistocene) of the soil is not taken into account. Liquefaction is very unlikely.

- The sample at El. +12.3 ft under the plant stack has a FOS = 1.0. This material may well be excavated based on final design (not yet determined).

- The remaining 4 samples are spread across the site and are not at locations of planned structures. The computed FOS ranges from 0.88 to 1.08. Soils in adjoining borings at similar depths had minimum FOS = 1.41.

To summarize, if very large numbers of soil samples are analyzed (e.g. 3,389 samples) across a large site, there will most probably be a few outliers with computed FOS values less than the stipulated minimum. In the case of the liquefaction analysis based on SPT results, 15 of the 3,389 samples had FOS < 1.1; this number was reduced to 6 when clay soils and excavated materials were taken into account. Only 2 of these had FOS < 1.0, and neither was under a planned structure.

There are no liquefiable zones based on SPT results and thus they cannot be shown as a graphical interpretation.

CPT Results

Table 2.5S.4-35 and Subsection 2.5S.4.8.2.3 summarize the results of liquefaction analyses using CPT results and tabulate boring locations and depths where the computed Factor of Safety (FOS) against liquefaction is < 1.1. The section states that 153 out of the 4,489 CPT results analyzed showed FOS < 1.1. As with the SPT results, the results reported in the table under the heading "Stratum (Disposition)" additionally take into account the soil type, and whether the soil will be excavated out during construction.

35 of the 153 samples were from areas to be excavated.

Of the remaining 118 results, 39 were from clayey soils (layers D and N (Clay)) which are very unlikely to liquefy.

Of the remaining 79 results, 66 were from areas where no structures are planned.

Of the remaining 13 results, only 2 had FOS <1.0, with the lowest being 0.95.

As noted with the SPT results, if very large numbers of CPT values are analyzed (e.g. 4,489 results) across a large site, there will most probably be a few outliers with computed FOS values less than the stipulated minimum. In the case of the liquefaction analysis based on CPT results, 153 of the 4,489 samples had FOS < 1.1; this number was reduced to 13 when clay soils, excavated materials and tests beneath no planned structures were taken into account. Only 2 of these had FOS < 1.0.

There are no liquefiable zones based on CPT results and thus they cannot be shown as a graphical interpretation.

No COLA revision is required as a result of this RAI response.

RAI 02.05.04-6:

<u>QUESTION</u>:

Table 2.5S.4-16, as well as the graphic boring logs, reveals that layer M was not sampled with the SPT and N-values, and soil property data do not exist for layer M. The properties from layer K were adopted for layer M according to Table 2.5S.4-16. However, the shear wave velocity measured in layer M is less than the shear wave velocity measured in layer K. Provide additional justification for assuming N-values and soil properties for layer M based on N-values and soil properties for layer K in light of these differences in shear wave velocities between the two layers.

<u>RESPONSE</u>:

The following values for various properties for layer M were considered:

Elastic Modulus, Shear Modulus and Shear Wave Velocity

In Table 2.5S.4-16, the geotechnical parameters denoting the high strain elastic and shear modulus values are not the same for layers M and K (Sand) since they are based partly on the shear wave velocity measurements. Similarly, the low strain shear modulus values are not the same since they are based entirely on shear wave velocity values, i.e.:

	Layer K (Sand)	Layer M
Elastic Modulus (high strain)	1,650 ksf	1,300 ksf
Shear Modulus (high strain)	650 ksf	500 ksf
Shear Modulus (low strain)	7,400 ksf	5,350 ksf
Shear Wave Velocity	1,370 ft/sec	1,165 ft/sec

SPT N-Value

The empirical relationship between high strain elastic modulus (E) and SPT N-value for sand can be expressed as:

$E = 36N$ ksf (Reference 1)

For E = 1,300 ksf (see above table for layer M), the equivalent N-value from the equation is 36 blows per foot (bpf). The corrected N-value for layer M (from layer K (Sand)) used in the FSAR is 30 bpf, which is slightly conservative based on the elastic modulus.

Angle of Internal Friction

Reference 2 indicates the angle of internal friction of dense sands with N-values of 30 or more in the 35 to 40 degree range. The angle of internal friction for layer M (from layer K (Sand)) in the

FSAR is 33 degrees. This is a somewhat conservative value compared to the value suggested in Reference 2.

Fines Content, Moisture Content and Unit Weight

The remaining 3 parameters in Table 2.5S.4-16 that are assumed to be the same for both layers K and M are the fines content (45%), moisture content (21%), and unit weight (127 pcf). These parameters are close in value to those of layer J (Sand), which has a shear wave velocity close to that of layer M.

Justification Summary

In summary, some of the layer M parameters used most frequently for engineering analysis (shear wave velocity, and elastic and shear modulus) are different from (and have smaller values than) those of layer K (Sand). Other parameters such as N-value and internal friction angle are lower than might be expected from a sand with a shear wave velocity of 1,165 ft/sec. The layer M parameters, which are assumed to be the same as those of layer K (Sand) (moisture and fines content and unit weight), are also similar to those of layer J (Sand). Thus, it is reasonable to assume that all three layers have similar properties even though there are differences in the shear wave velocities.

No COLA revision is required as a result of this RAI response.

References:

1. Davie, J.R. and M.R. Lewis. "Settlement of Two Tall Chimney Foundations," Proceedings, Second International Conference on Case Histories in Geotechnical Engineering, pp. 1309-1313, St. Louis, MO, June 1988.

2. Bowles, J.E., “Foundation Analysis and Design,” Third Edition, McGraw-Hill Book Company, New York, 1982.

RAI 02.05.04-7:

QUESTION:

Figures 2.5S.4-29 and 2.5S.4-30 show overconsolidation ratios (OCR) derived from CPT test data at shallow depths (El. 30 ft to El. -70 ft). The calculated OCR values vary significantly in the various clay layers, but show a general trend of decreasing OCR with depth. Below El. -61 ft the OCR range varies from less than 1.0 to 3.0. You used an average OCR of 1.8 to represent this depth interval (Strata F and J). However, the CPT data indicate a trend of decreasing OCR below El. -60 ft, with some data points indicating OCR values of less than 1. Consolidation data do not show this trend. Please reconcile the different results and justify the assumed OCR value of 1.8 given the observed CPT trend of decreasing OCR below El. -60 ft.

RESPONSE:

The definition of OCR is the maximum past pressure divided by present overburden pressure. In most soil profiles, the OCR decreases with increasing depth, eventually reaching unity or very close to unity, where the maximum past pressure is slightly greater than or equal to the present overburden pressure. Thus the trend of decreasing OCR with depth at the STP COL site is expected.

The OCR values in the plots of OCR versus elevation on Figures 2.5S.4-29 and 2.5S.4-30 are computed using a third order equation that involves the undrained clay shear strength derived from the recorded cone tip resistance. (These undrained shear strengths are shown on Figures 2.5S.4-23 and 2.5S.4-24.) A reasonable amount of scatter can be expected using this empirical equation, and thus occasional OCR values of less than 1 can result. However, the average values on Figures 2.5S.4-29 and 2.5S.4-30 can be considered to be representative of the OCR values derived from the cone penetration test (CPT) results. (Note that there is no geologic mechanism for Pleistocene-age samples to have an OCR less than 1, i.e., present effective overburden pressure greater than the maximum past pressure. Thus, the occasional values of OCR < 1 in Figures 2.5S.4-29 and 2.5S.4-30 are outliers that most probably result from the cumulative effects of using the empirical equations to compute OCR and undrained shear strength, as noted above.)

Referring to Figures 2.5S.4-29 and 2.5S.4-30, the average OCR values from the CPT for Stratum F are 1.8 for STP 3 and 2.5 for STP 4, giving a rounded-up average of 2.2 (as shown on Table 2.5S.4-13). From Table 2.5S.4-13, the average OCR from consolidation tests on Stratum F is 2.9. From Table 2.5S.4-13, the OCR value selected for engineering use for Stratum F is 2.6.

As illustrated on Figure 2.5S.4-30, the average OCR value from the CPT for Stratum J (Clay) is 1.8 for STP 4. No CPT results were measured in Stratum J (Clay) for STP 3. Thus the average CPT value of OCR in Stratum J (clay) given in Table 2.5S.4-13 is 1.8. From Table 2.5S.4-13, the average OCR from consolidation tests on Stratum J (Clay) is 1.9. From Table 2.5S.4-13, the OCR value selected for engineering use for Stratum J (Clay) is 1.7.

In summary, because of the definition of OCR, in most soil profiles the OCR decreases with increasing depth, eventually reaching unity or very close to unity. As shown in the "Selected Values for Engineering Use" portion (extracted and shown below) of Table 2.5S.4-13, the OCR values selected at STP follow this trend:

Stratum	A	D	F	J Clay	K Clay	L	N Clay
OCR	7.0	3.3	2.6	1.7	1.3	1.0	1.0

No COLA revision is required as a result of this RAI response.

RAI 02.05.04-8:

<u>QUESTION</u>:

Figure 2.5S.4-28 shows that the OCR computed from consolidation tests falls below 1.0 at or below El. -270 ft. The liquidity indices shown in Figure 2.5S.4-20 do not indicate near normally consolidated or under-consolidated layers below this depth. Please reconcile the difference in the interpretation of these data and explain how the consolidation data were used in computing settlements.

<u>RESPONSE</u>:

Considering the definition of overconsolidation ratio (OCR) (maximum past effective pressure divided by present effective overburden pressure), in most soil profiles the OCR decreases with increasing depth, eventually reaching unity or very close to unity. Thus the trend of decreasing OCR with depth at the STP COL site is expected. At a depth of El. -270 ft, the effective vertical overburden pressure is close to 20 ksf. Therefore, even with an OCR = 1, the soil has an effective preconsolidation pressure of 20 ksf, and is thus highly consolidated, with a typically low natural moisture content due to the consolidation process. Thus, the plots on Figure 2.5S.4-20 that show a very low liquidity index, i.e., the natural moisture content is very close to the plastic limit, could still indicate soils that are normally consolidated or close to normally consolidated.

Although the OCR of very deep samples typically approaches unity, i.e., the preconsolidation pressure will plot at or a little above the Effective Overburden Pressure line shown on 2.5S.4-28, these samples should not plot below the line, since there is no geologic mechanism for Pleistocene-age samples to have a present effective overburden pressure greater than the maximum past pressure. The explanation for the two deep points lying below the Effective Overburden Pressure line shown on 2.5S.4-28 is most probably that these deep samples suffered disturbance due to pressure relief on being extracted from very high confining pressures below 300 ft depth. This type of disturbance usually results in a flattening of the void ratio versus log pressure curve, leading to an underestimation of maximum past pressure.

Elastic parameters were used to estimate settlement in all of the settlement calculations, except when considering layer L at around El. -230 ft. This layer was estimated to have an OCR = 1, and so any applied loading to the layer was computed as virgin consolidation. Layer L is only about 5 ft thick, and so the maximum computed virgin compression settlement beneath any structure was less than ¼ inch.

No COLA revision is required as a result of this RAI response.